AGING RESPONSE OF AZ SERIES MAGNESIUM ALLOYS AFTER THERMO-MECHANICAL PROCESSING

A Thesis

by

Mustafa Mısırlı

Submitted to the
Graduate School of Sciences and Engineering
In Partial Fulfillment of the Requirements for
the Degree of

Master of Science

in the
Department of Mechanical Engineering

Özyeğin University
August 2019

AGING RESPONSE OF AZ SERIES MAGNESIUM ALLOYS AFTER THERMO-MECHANICAL PROCESSING

Approved by:

Assoc. Prof. Dr. Güney Güven YAPICI,
Advisor,
Department of Mechanical Engineering
Head of Department
Özyeğin University

Assist. Prof. Dr. Alpay ORAL
Department of Mechanical Engineering
Yıldız Technical University

Assist. Prof. Dr. Altuğ BAŞOL,
Department of Mechanical Engineering
Özyeğin University

Date Approved: 20 August 2019

DEDICATION

To my wife and daughter

ABSTRACT

The current study aims to investigate the effect of thermo-mechanical treatment utilizing both aging and stress aging on the mechanical behavior of warm rolled AZ31 magnesium alloy with inspecting the relationship between the microstructure evolution, tensile properties, and fracture morphology.

The individual contributions of conventional and stress aging on the tensile properties and microstructure of the warm rolled AZ31 magnesium alloy are investigated in detail. The aging treatments were conducted at different temperatures of 120˚C and 180˚C for various durations ranging from 1h to 48h. Annealed AZ31 magnesium alloy was used as the as-received slab and homogenization treatment was conducted at 400˚C for 3h before the rolling process.

Inspection of tensile test results revealed that the ultimate tensile strength (UTS) of the as-received AZ31 after 24h aging at 120˚C increased up to 300 MPa with a 2% reduction in failure strain. Whereas the yield strength (YS) of the specimen aged at 180˚C for 24h decreased to 190 MPa with the improvement of ductility near to 14% and the UTS up to 285 MPa. Also, stress aging at 120 ˚C for only 1h after rolling, increased the yield strength of the as-received sample to over 240 MPa.

Microstructural observations displayed that the grain growth initially diminished the strength of rolled samples while improving the ductility. This is followed by the nucleation of recrystallized grains which improves the ultimate strength with satisfactory ductility as compared to the rolled specimens. Furthermore, the fracture morphology of stress aged samples presents nucleation-controlled fracture mechanisms with deeper void structures as a common ductile characteristic.

It was also demonstrated that the utilization of stress aging process and thereby affecting the precipitation kinetics, a microstructure can be achieved with high level of yield strength and acceptable ductility. Also, treatment duration of stress aging process is much lower than the conventional aging and it can be an important factor for efficient utilization of resources in industrial applications. Moreover, the thermal conductivity of stress aged sample at 120˚C for 1h was increased up to about 99 W/mK which may be attributed to the existence of favorable precipitate formations during stress aging.

ÖZETÇE

Bu çalışma, yaşlanma ve gerilme yaşlanmasından faydalanan termo-mekanik işlemenin, ılık haddelenmiş AZ31 magnezyum alaşımının mekanik davranışı üzerindeki etkisini, mikroyapı gelişimi, çekme altında özellikleri ve kırılma morfolojisi arasındaki ilişkiyi inceleyerek araştırmayı amaçlamaktadır.

Geleneksel ve gerilme yaşlanmasının, ılık haddelenmiş AZ31 magnezyum alaşımının gerilme özelliklerine ve mikroyapısına katkıları ayrıntılı olarak incelenmiştir. Yaşlanma işlemi, 1 saat ila 48 saat arasında değişen süreler için 120°C ve 180°C olan farklı sıcaklıklarda gerçekleştirildi. Tavlanmış AZ31 magnezyum alaşımı, işlem görmemiş levha olarak kullanıldı ve homojenizasyon işlemi, haddeleme işleminden önce 3 saat 400°C'de gerçekleştirildi.

Çekme testi sonuçlarının incelenmesi, 120°C'de 24 saat yaşlandırılılma sonrası elde edilen AZ31'in maksimum çekme dayanımının, kırılma uzamasında % 2'lik bir azalmaya karşın 300 MPa'ya yükseldiğini ortaya koymuştur. 180°C'de 24 saat boyunca yaşlanma işlemi uygulanan numunenin akma dayanımı, % 14 kadar sünekliliğinin iyileşmesi ile 190 MPa'ya düşmüştür ve çekme dayanımı 285 MPa'ya kadar yükselmiştir. Ayrıca, haddelenmiş numunenin 120˚C'de sadece 1 saat uygulanan gerilme yaşlanması nedeniyle işlem görmemiş numuneye göre akma dayanımını 240 MPa'nın üzerine çıkarmıştır.

Mikroyapısal gözlemler, tane büyümesinin başlangıçta sünekliği geliştirirken, haddelenmiş numunelerde yumuşama meydana getirdiğini göstermiştir. Bu durum, haddelenmiş numunelere kıyasla tatmin edici süneklikle beraber çekme dayanımını geliştiren yeniden kristallenmiş tanelerin çekirdeklenmesiyle takip edilmiştir. Ayrıca,

gerilme yaşlanması uygulanmış numunelerin kırılma morfolojisi ortak bir sünek karakteristik olarak derin boşluklu yapılara sahip çekirdeklenme kontrollü kırılma mekanizmaları sunmaktadır.

Ayrıca, numunelerde gerilme yaşlanma işlemi kullanıldığında çökelme sertleşmesi kinetiklerine etki edilerek, yüksek akma dayanımı ve kabul edilebilir süneklik seviyesine sahip bir içyapı elde edilebildiği gösterilmiştir. Ayrıca, gerilim yaşlanması işleminin etki süresi, geleneksel yaşlanmaya göre çok daha düşüktür ve endüstrideki kaynakların verimli kullanımı için önemli bir faktör olabilir. Ayrıca, 1 saat boyunca 120˚C'de gerilme yaşlanması uygulanmış numunenin termal iletkenliği, gerilme yaşlanması sırasında uygun çökelti yapısı oluşumu ile 99 W/mK seviyesine yükseltilmiştir.

ACKNOWLEDGMENTS

First and foremost, I would like to thank my supervisor, Dr. Güney Güven Yapıcı, for his wonderful guidance and limitless support throughout the course of my research work. I am indebted to him for his continual encouragement and support to carry out the current study.

On the other hand, I would like to thank my MSc. committee members, Assist. Prof. Dr. Alpay Oral and Assist. Prof. Dr. Altuğ Melik Başol for their guidance and attention to this study.

Special thanks go to my friend Ali Hosseinzadeh Ghobadlou who has made valuable help and suggestions during my master education.

I highly appreciate my wife and my parents, who dedicated their lives to support me throughout my school and university years.

Finally, I would like to acknowledge Vestel Company for giving me this opportunity.

TABLE OF CONTENTS

LIST OF TABLES

LIST OF FIGURES

1 INTRODUCTION

1.1 Motivation

Magnesium is not only the sixth most plentiful element on the Earth's crust but also the third most abundant element dissolved in seawater, with an estimated concentration of 0.14%. Recently, magnesium alloys especially AZ series, are suitable nominates for structural components, as an alternative material for heavier aluminum and steel. These alloys represent noteworthy properties such as high strength to weight ratio, good corrosion resistance, low density, along with good machinability, weldability, and castability, etc. Nevertheless, low formability of magnesium alloys restricts processing such as rolling, extrusion, and metal forming and consequently, it limits their applications in industry.

The major reason for the low formability is the insufficient slip and twinning systems in the hexagonal close-packed (HCP) crystal structure of magnesium alloys at room temperature. Critical resolved shear stresses (CRSS) levels have been determined for separate slip and twinning systems of magnesium alloys. The CRSS level of the basal slip is very lower than the non-basal and twinning modes, which provides only two independent slip modes for HCP magnesium, while the deformation of the material requires additional activation of twins and non-basal systems.

Many works have been applied to the advancement of thermomechanical treatment processes for developing the mechanical properties of magnesium alloys to eliminate the formability limitation and spread the range of their applications. Warm rolling followed by post heat treatment is one of the most common methods for improving the mechanical properties of magnesium alloys.

One of the most important aim of this work was improving the processing capability and formability of a lightweight magnesium alloy to substitute with the heavier materials in the industry. Additionally, high thermal conductivity of material after processing can be enhance the applicability of the final product in many cases, which is considered in this investigation.

However, magnesium alloys do not have a suitable age-hardening response in comparison with aluminum alloys, due to the lower amount of precipitates. In spite of the previous researches about the warm rolling followed by age hardening of magnesium alloys, there is a lack of study concerning the influence of external stress during aging on the mechanical properties of AZ31.

1.2 Research objectives

The main aim of the current study is investigating the influence of thermo-mechanical treatment utilizing both aging and stress aging on the mechanical characteristics of warm rolled AZ31 magnesium alloy with inspecting the relationship between the microstructure evolution, tensile properties, and fracture morphology. Theoretical and experimental investigations are specially employed to examine the effect of temperature and duration of aging on the mechanical behavior of rolled slabs materials and fracture mechanisms.

1.3 Work summary

The individual contributions of conventional and stress aging on the tensile properties and microstructure of the warm rolled AZ31 magnesium alloy are investigated in detail. The aging treatments were conducted at different temperatures of 120˚C and 180˚C for various durations ranging from 1 h to 48 h. Annealed AZ31 magnesium alloy

was used as the as-received slab and homogenization treatment was conducted at 400˚C for 3h before the rolling process.

Inspection of tensile test results revealed that the ultimate tensile strength (UTS) of the as-received AZ31 after 24 h aging at 120˚C increased up to 300 MPa with a 2% reduction in failure strain. Whereas the yield strength (YS) of the specimen aged at 180˚C for 24 h decreased to 190 MPa with the improvement of ductility near to 14% and the UTS up to 285 MPa. Also, stress aging at 120 ˚C for only 1h after rolling, increased the yield strength of the as-received sample to over 240 MPa.

Microstructural observations displayed that the grain growth initially diminished the strength of rolled samples while improving the ductility. This is followed by the nucleation of recrystallized grains which improves the ultimate strength with satisfactory ductility as compared to the rolled specimens. Furthermore, the fracture morphology of stress aged samples presents nucleation-controlled fracture mechanisms with deeper void structures as a common ductile characteristic.

2 BACKGROUND AND LITERATURE REVIEW

2.1 Properties of Pure Magnesium

The place of magnesium on the periodic table is under the alkaline earth metal group. It's group number 2 and it is under the same group with Be, Ca, Sr, Ba, and Rd [1]. The atomic properties of magnesium are given in Table 2.1.

Table 2.1 Atomic properties of magnesium.

Element Symbol	**Mg**
Atomic Number	12
Atomic Weight	24.3050
Atomic Diameter	0.320 nm
Atomic Volume	14.0 cm3/mol

The density of magnesium is 1.74 g/cm3. Comparing with other structural engineering materials like aluminum (SP:2.7 g/cm3) and iron (SP:7.86 g/cm3), magnesium is one of the lightest structural metal [2, 3]. This advantage of magnesium and magnesium alloys makes an appropriate selection for different engineering applications. Physical properties of magnesium, aluminum, and iron are given in Table 2.2.

Table 2.2 Physical properties of Mg, Al, and Fe.

Property	Magnesium	Aluminum	Iron
Crystal structure	HCP	FCC	BCC
Density at 20°C (g/cm^3)	1.74	2.70	7.86
Coefficient of thermal expansion 20–100°C (×10^6/C)	25.2	23.6	11.7
Elastic modulus (10^6 MPa)	44.126	68.947	206.842
Tensile strength (MPa)	240 (for AZ91D)	320 (for A380)	350
Melting point (°C)	650	660	1536
Thermal conductivity at 20°C (W/mK)	170	225	71.9

As shown in Figure 2.1, Magnesium's crystal structure is a hexagonal close-packed structure (hcp) and its atomic diameter is 0.320 nm. The stacking layers arranged as ABAB in a cell unit. At room temperature, a and c values for magnesium are a = 0.32092 nm and c = 0.52105 nm. The c/a value is 1.6236 and it's almost the same as the ideal value of 1.633, that is making the magnesium to preferred metal for a solid solution with various metals like Zn, Al, Zr, etc [4].

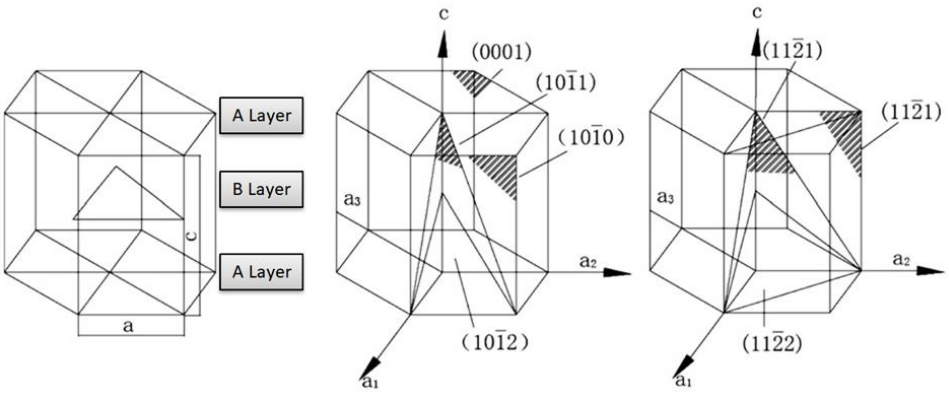

Figure 2.1 Layers of the hexagonal close-packed (HCP) structure and important planes and directions in the HCP.

Due to the hcp crystal structure of the magnesium, the restricted number of the slip systems causes difficulties to its deformation mechanism at the ambient temperature. The mechanical test results reveal that pure magnesium's mechanical properties are not suitable for structural material. A most common method for improving the mechanical properties of magnesium is alloying it with various types of metals. Also, there are different types of methods to enhance the mechanical behavior of magnesium after alloying such as precipitate hardening and grain refinement.

2.2 Magnesium Alloys

Currently, there is no available international system for classification and designation of Mg alloys. Therefore, American Society for Testing Materials (ASTM) has a description for this issue. According to ASTM, in the first part, the designation of mg alloys are made by letter codes of two major alloying elements and the second part includes a two-digit number of those two elements' weight percentages [5]. Some of the designation examples for mg alloys are given in Table 2.3.

Table 2.3 Designation examples for mg alloys.

Examples	Elements	Composition (wt.%)
AZ31	Aluminum (A), Zinc (Z)	3Al-1Zn
ZC71	Zinc (Z), Copper (C)	7Zn-1Cu
ZK30	Zinc (Z), Zirconium (K)	3Zn-0.6Zr
AM60	Aluminum (A), Manganese (M)	6Al-0.13Mn
AS41	Aluminum (A), Silicon (S)	4.3Al-1Si

Also for the heat treatment designation of magnesium alloys, there are a letter or a letter and few-digit numbers which are explained following condition. (F) is the letter is using for as-fabricated, (O) letter for annealed, (H) letter for strain hardened, (T) letter for tempered and (W) letter for solution heat treated. The digit(s) explain the type of heat treatment. The usually used type of heat treatments are (T4) for solution treated, (T5) for direct cooling and artificially aged, and (T6) for solution treated and artificially aged. The widely used alloy materials and their codes for magnesium are aluminum (A), zinc (Z), zirconium(K), rare earth elements (E), copper (C), silicon (S), manganese (M), yttrium (W), thorium (H), lithium (L) and silver (Q)[5].

The most common type of strengthening for magnesium alloys is the solid solution strengthening according to their atomic properties and lattice parameters mentioned in previous sections. Different alloying elements can enhance different mechanical properties of magnesium.

Aluminum (Al) gives more ductility and strength to a magnesium element. The addition of 6 wt% Al gains optimum strength and ductility to magnesium. Up to 12.7 wt% Al can be found in Mg and increase the al weight in magnesium alloys provides more castability to alloy. Zinc (Zn) is one of the most commonly used solid solution strengthener for mg alloys. It also decreases negative effects of Ni or Fe impurities for corrosion resistance of magnesium alloys. In addition to this, zinc can be added to other mg alloys to improve their age-hardening characteristics.

Zirconium (Zr) is using for grain refiner in Mg. It's lattice parameters almost same with Mg (Zr, a = 0.323 nm, c = 0.514 nm / Mg, a = 0.32 nm, c = 0.52 nm). Rare Earth (RE) Elements which are Neodymium (Nd), Cerium (Ce), Lanthanum (La), Gadolinium (Gd) and Praseodymium (Pr) are using for enhancing the creep strength of magnesium

alloys. They provide stable grain boundaries and perform restriction to grain boundary sliding.

Transition Elements which are copper (Cu), iron (Fe), nickel (Ni) and cobalt (Co) are using for corrosion resistance of magnesium alloys. The tolerance limit of Cu, Fe, and Ni are 0.05 wt% Cu, 0.005 wt% Fe and 0.005 wt% Ni. Silicon (Si) is helping for improvement of the fluidity of molten Mg alloys. Manganese (Mn) does not affect to Mg directly but it associates with detrimental heavy elements (e.g. Fe) and turning them to harmless intermetallic in Mg-Al and Mg-Al–Zn alloys [6].

Yttrium (Y) is combined with rare-earth (RE) elements to improve creep resistance and high-temperature strength. Thorium (Th) is used for creep resistance and improve castability. Thorium is no longer used because it is a radioactive element. Lithium (Li) is the only element to use for reducing the density of magnesium alloys. Also, the effect of addition Li to mg alloys reduces strength but improves ductility [7].

2.3 AZ31 magnesium alloy

This investigation focuses on the development of mechanical properties of AZ31 magnesium alloy which is a member of Magnesium-Aluminum-Zinc-Manganese (AZ) alloy system. Commonly used magnesium alloy systems are Magnesium-Manganese, Magnesium-Aluminum-Zinc-Manganese, Magnesium-Aluminum-Manganese, Magnesium-Rare Earth Metal-Zirconium, Magnesium-Zinc-Zirconium, Magnesium-Zirconium, Magnesium-Silver-Rare Earth Metal-Zirconium, Magnesium-Yttrium-Rare Earth Metal-Zirconium. The most important and widely used magnesium alloy system is the AZ series. The Mg-Al- Zn alloy system is found in 1913 [8].

Since its discovery, this alloy system has been developed by many researchers. For example, in the beginning, Mg-Al-Zn used widely in Germany but their usage areas

are limited due to their corrosion problem in the wet environment. In 1925, this issue is handled by learning of manganese addition to Mg-Al-Zn alloy. The addition of manganese can enhance the corrosion resistance of the alloys [9].

Magnesium AZ31 alloy can be found in different forms such as plate, sheet, and bar. It is an alternative to aluminum alloys due to its high strength to weight ratio. It has very high machinability rating and good forgeability. AZ Series also commonly used for the areas which require good castability.

2.4 Deformation mechanisms of magnesium alloys

According to hexagonal close-packed (hcp) crystalline structure and melting point (650 °C) of pure magnesium, it has limited slip basal planes at ambient temperature. That is giving it difficult plastic deformability and low ductility at ambient temperature [10]. Additional slip systems of magnesium alloys can be activated by elevating the temperature. Magnesium alloys can be better formed below 227 °C, generally in the range of 343 to 510 °C [11].

The main deformation mechanism for magnesium alloys is basal slip system at room temperatures. Also, twinning is a deformation mechanism for mg alloys when slip systems are required for deformation. At high temperatures, grain boundary sliding (GBS) can be the primary deformation mechanism of magnesium alloys [12, 13].

2.4.1 Slip systems

Plastic deformation of crystalline materials usually occurs by slip. The slip is the displacement of a plane of one part of a crystal to over another crystal by dislocation movements under the influence of shear forces. The planes that occur slip are called slip planes and the direction of slip termed slip direction. These properties define the

characteristic of the crystal structure of materials. The slip planes and the slip directions combined to termed the slip systems. The direction of the dislocation has to be the easiest direction in which the density of atoms is the highest [14].

Slip systems defined with a combination of these slip planes and directions. The highest atomic density plane of magnesium structure is (0001) plane (basal plane), and the slip direction is {11-20}. Magnesium slip systems, twinning plane, and directions were schematically illustrated in Fig. 2.2.

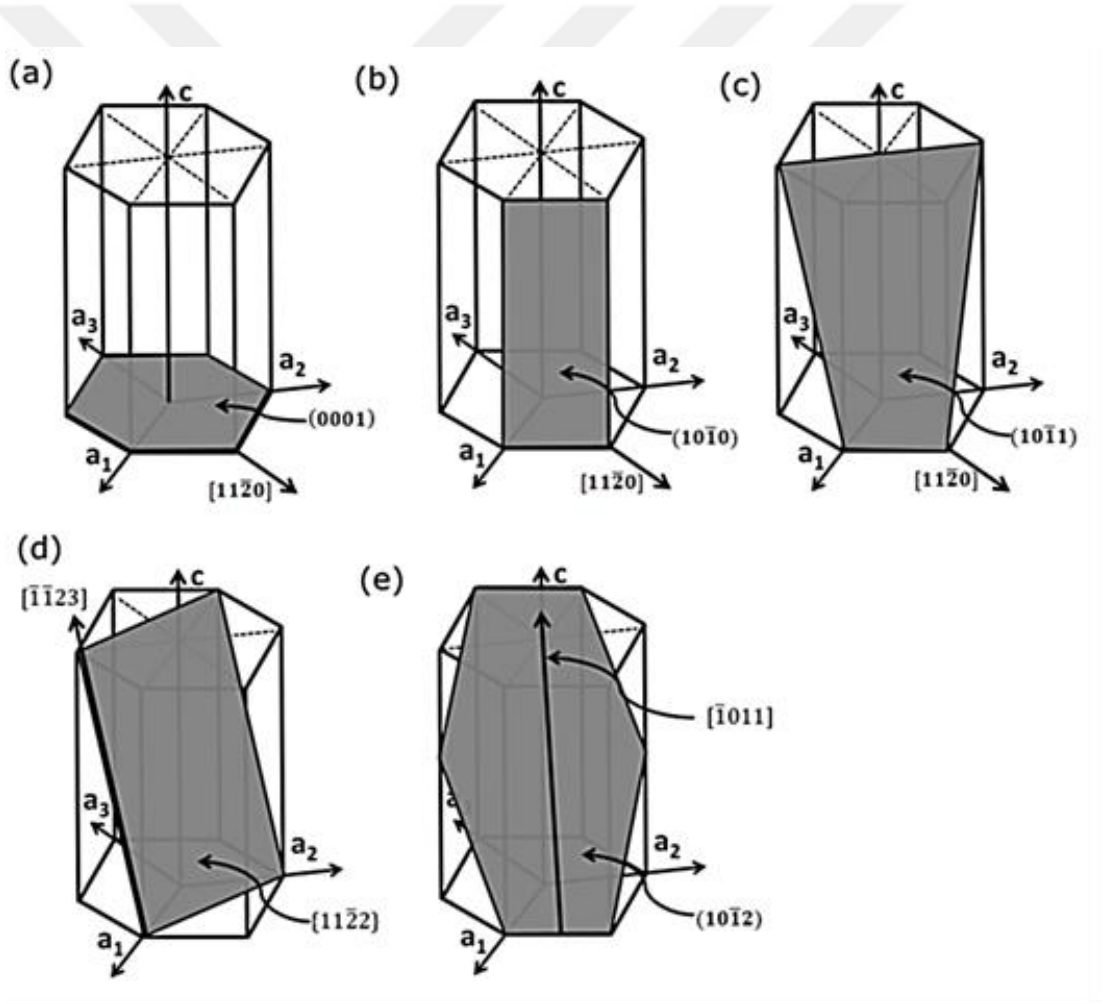

Figure 2.2 Slip and twinning systems in a magnesium crystal (a) basal (0001) {11-20} (b) prismatic (10-10) {11-20} (c) first-order pyramidal (10-11) {11-20} (d) second-order pyramidal (11-22) {1123} slip systems (e) tension twinning (10-12){10-11}.

According to the Von-Mises yield criterion, Uniform deformation needs at least five active independent slip system [15, 16]. The HCP structure has three classes of slip system these are basal, prismatic, and pyramidal. In magnesium, the critical resolved shear stress (CRSS) for the basal slip is less approximately one hundred times than pyramidal and prismatic planes that show, the two independent basal slip systems are weak for the uniform yielding criterion [17]. The independent slip systems in hcp structure with the number of slip systems, name of the planes, and Burgers vector type are listed in Table. 2.4.

Table 2.4 Independent slip systems in HCP metals [18].

Slip System	Burgers vector type	Slip direction	Slip plane	No of slip system	
				Total	Independent
1	a	<11-20>	Basal (0001)	3	2
2	a	<11-20>	Prism type I {10-10}	3	2
3	a	<11-20>	1^{st} – order pyramidal type I {10-11}	6	4
4	c+a	<11-23>	2^{nd} – order pyramidal type II {11-22}	6	5

Fig. 2.3 demonstrates the effect of temperature on the critical resolved shear stress (CRSS) of different slip systems of hcp structure for magnesium alloys. The independency of basal and twinning is obvious while the CRSS of the prismatic and

pyramidal slip systems is decreasing with increasing the temperature from ambient temperature up to 500˚C.

The main slip system of magnesium alloys is the basal system which has a CRSS of 0.6-1MPa. The second possible system of deformation is twinning with the CRSS of about 2.8MPa and the rest of them are relatively inactive at ambient temperature. But as shown in Fig. 2.3 with increasing the temperature up to 500 the CRSS values of prismatic and pyramidal slip systems were decreasing to 1MPa and 2MPa, respectively.

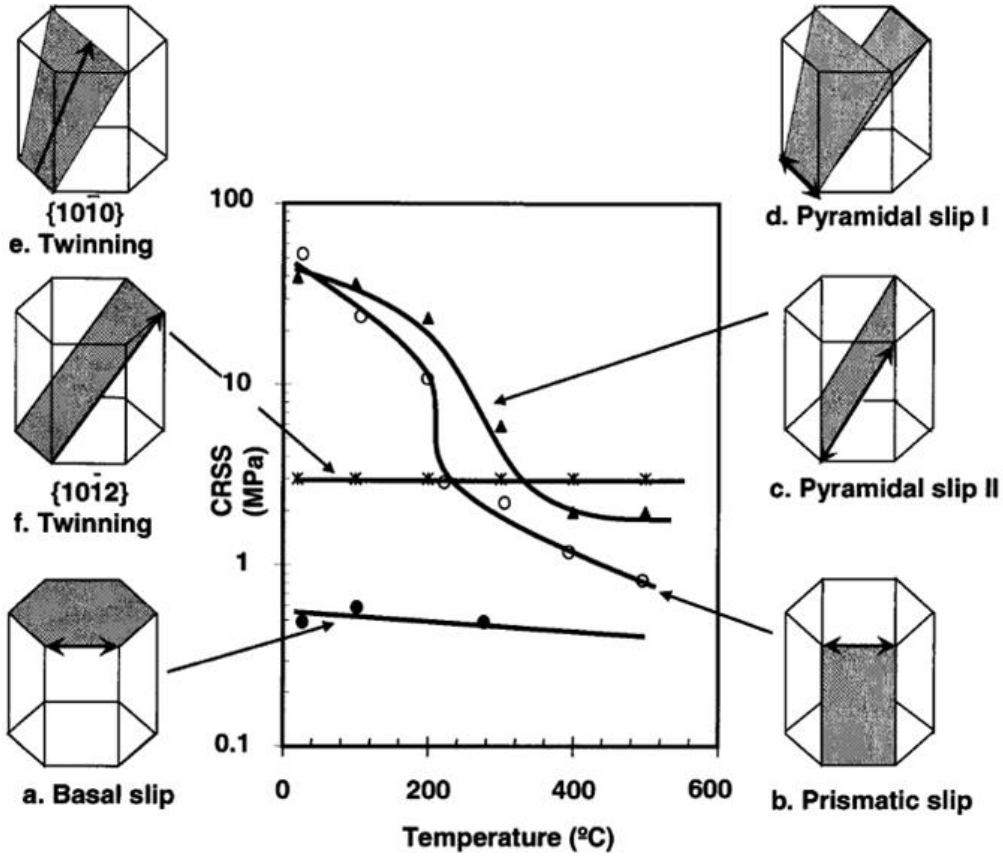

Figure 2.3 Principal slip systems and twinning: (a) basal slip system, (b) prismatic slip system, (c) second order pyramidal slip system, (d) first order slip systems, (e) twinning {10-10}, and (f) twinning {10-12} [19].

2.5 Deformation by twinning

In addition to slip systems, Magnesium and magnesium alloys can deform by twinning when the slip systems are required. Twinning is, in a deformed metal, crystal structure shows mirrored portion in respect of a plane. Rest of the metal, within the undeformed structure, shows an untwined crystal structure. The symmetry plane between the two portions is called the twinning plane [20].

The twinning behavior can change according to grain size, strain rate, temperature, chemical composition and initial texture on Mg alloys [21]. Grain orientation and loading direction define the twinning deformation [22]. Previous studies show that the types of mechanical twinning are contraction, $\{10\bar{1}1\}\ \langle 10\bar{1}\bar{2}\rangle$, extension, $\{10\bar{1}2\}\langle 10\bar{1}\bar{1}\rangle$, and double twinning, $\{10\bar{1}1\}-\{10\bar{1}2\}$. Twinning deformation is the only active deformation that gives straining along the c-axis of the HCP crystalline structure at room temperature. Based on previous studies, mechanical properties of magnesium alloys (such as ductility) can enhance by dynamic recrystallization and grain reorientation [23, 24].

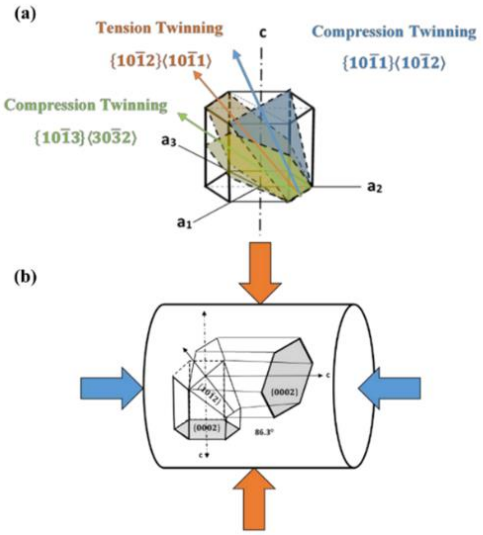

Figure 2.4 Deformation twinning in hcp structure. (a) extension, compression twinning and (b) schematic of loading path for the activation of twinning [25].

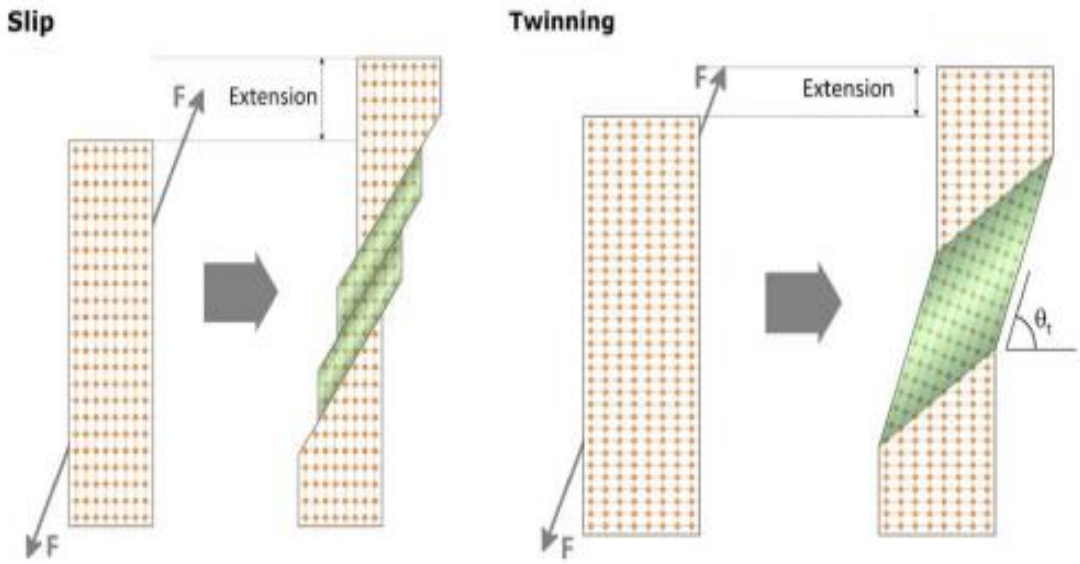

Figure 2.5 Schematic of slip and twinning in a face-centered cubic crystal [26].

Slip occurs when dislocations glide through the material, causing crystal planes to slide along each other. Twinning occurs via a concerted shift of atomic positions in the twinning direction. The twin crystal's structure is a mirror image of the parent structure about the twinning plane.

2.6 Texture

In general usage, "texture" word is using for physical patterns on a woven fabric. In material science, texture means the orientation of grains or crystals inside the polycrystalline material. Also, texture defines the preferred orientation of grains in polycrystals in literature. The improvement of the texture can change the deformation behavior of the material. On the other hand, the deformation process, such as rolling, effects to grains orientations of polycrystalline material that is affects to change material properties like mechanical and thermal properties. Texture can investigate with diffraction techniques. Pole figures are using for describing the texture with two-dimensional illustrations (Fig.2.6) [27].

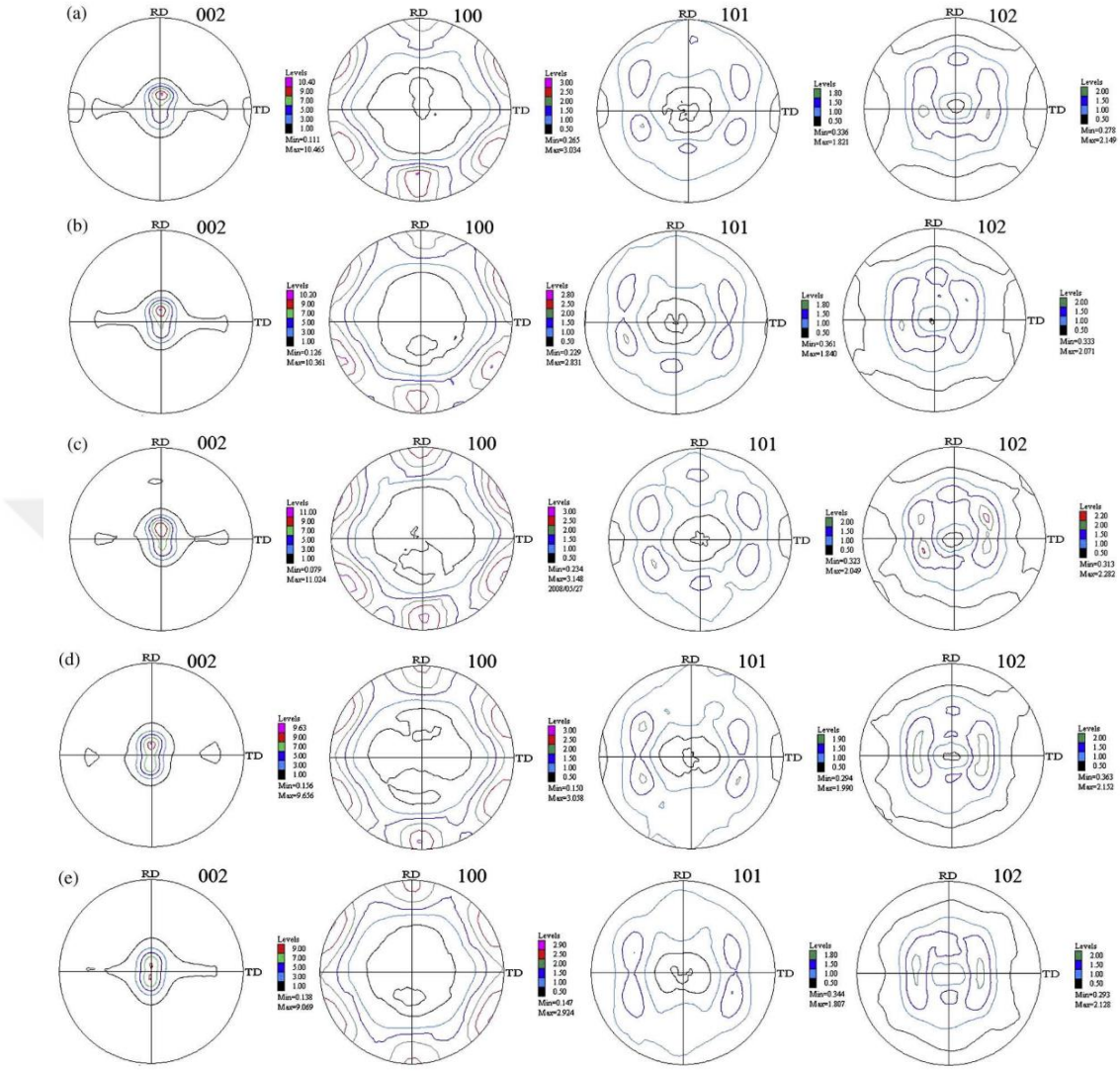

Figure 2.6 The (0002), (10–10), (10–11) and (10–12) pole figures of AZ31 magnesium sheets produced by (a) hot extruding and (b)9%, (c)16%, (d)22%, (e)25% rolling at room temperature [28].

At the moment of the rolling process of magnesium alloys, the strong basal texture is occurring and that shows us, grains basal planes orientation are parallel to the RD (rolling direction). Also, At the rolled samples which have basal texture, grain's <c> axis is parallel to the ND (normal direction of rolling).

2.7 Recrystallization in magnesium alloys

Grain refinement is one of the most important processes for the improvement of mechanical properties of materials. Recrystallization is one stage of grain refinement and to understand recrystallization, all of the stages of grain refinement which are cold working, recovery, recrystallization, and grain growth are shown in Fig. 2.7.

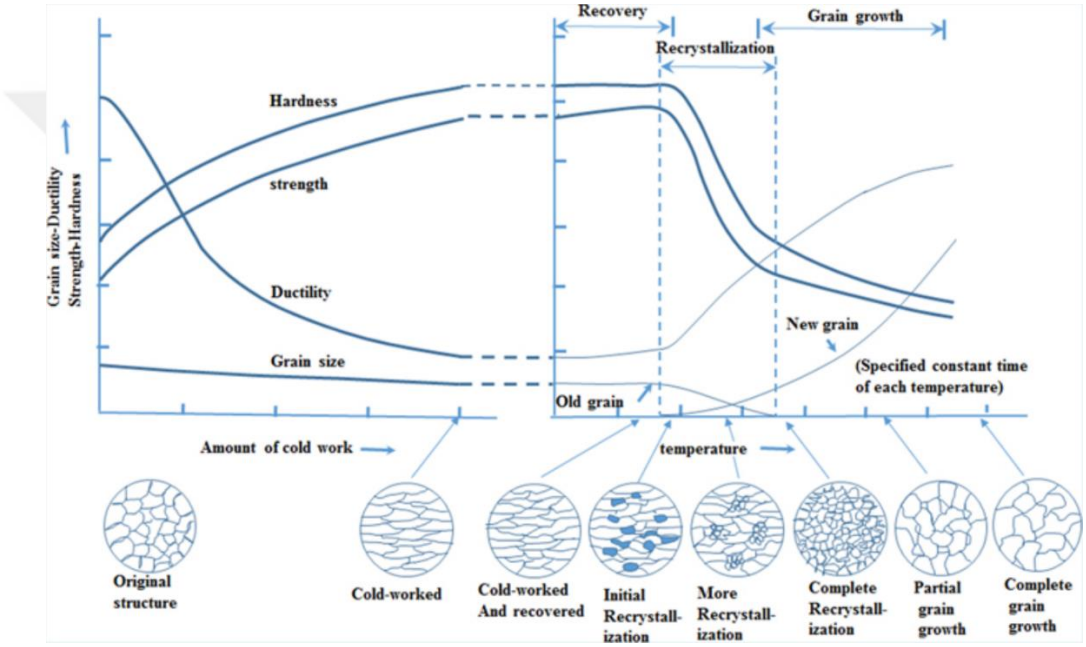

Figure 2.7 Different stage of grain refinement [29].

During the cold working process such as rolling, if the applied external load exceeds the yield strength of the material, dislocations start to move to the grain boundary. These dislocations produce back pressure which is calling as residual stresses and this back pressure becomes an obstacle for the movements of dislocation. Because of grain deformation and back pressure, the material's internal energy has increased. Recovery, recrystallization and grain growth mechanisms are used for reducing this internal energy of the material.

The recovery process is aimed to partially restore of properties changes of deformed material before deformation. Due to cold working, the dislocations on grain boundary which produce back pressure have changed the properties of the material. The annealing process is used to reduce and reorientation of these dislocations. During the Annealing process, dislocation's movability is increased by high temperature.

As shown in Fig. 2.8 when the dislocations which have opposite sign match, the effects of these dislocations and the contribution of these dislocations to the internal energy are removed themselves. Remain dislocations are reoriented themselves in a regular pattern and as a result of this orientation, residual stresses are relieved [30].

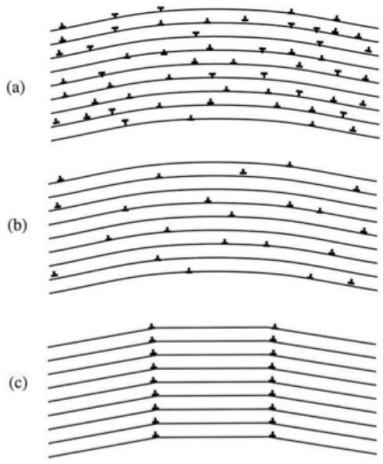

Figure 2.8 Recovery by polygonization of a bent crystal includes edge dislocations (a) as deformed, (b) after dislocation annihilation, and (c) tilt boundaries formation [31].

After that with further heating, new equiaxed small grains form and substitute the original grain structure. The varıatıon of internal energy of strained and unstrained material acts as a driving force in the aforementioned mechanism. This new microstructure has more limited dislocation density. The range of recrystallization depends on the temperature and duration of heat treatment. Also, recrystallization is known as the process of grain refinement.

2.8 Thermo-mechanical processes of Mg Alloys

At room temperature, magnesium and its alloys have weak formability due to their limited slip systems of hcp microstructure. Many researchers tried to improve mechanical behaviors of magnesium and its alloys with thermomechanical processes. The common thermomechanical methods for grain refinement of the magnesium alloys are accumulative roll bonding (ARB) [32, 33], hot and cold rolling [34], high-pressure torsion (HPT) [35, 36], and equal channel angular pressing (ECAP) [37, 38]. All these methods aimed to reduce grain size and redefine the microstructure of magnesium alloys.

Accumulative roll bonding (ARB) enhances the mechanical properties of Mg-Al alloys by reducing grain size with an efficient and low-cost way. In this process, Mg alloy samples are rolled by a determined reduction percentage according to the number of cut of the rolled sample. These rolled and cut magnesium alloy slabs are stacking by overlapped and then roll again. Homogeneous microstructures can be produced by increasing the quantity of the rolling passes [39]. The accumulative roll bonding (ARB) process is shown in Fig. 2.9.

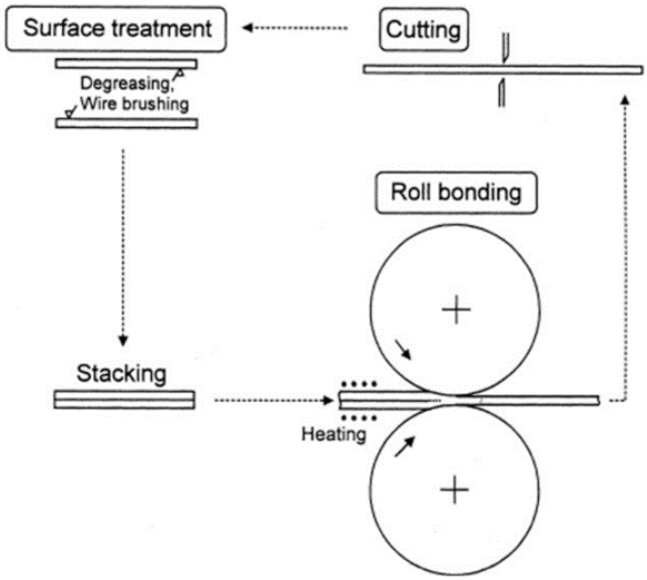

Figure 2.9 Accumulative roll bonding (ARB) process [40].

The most common and efficient methods for grain refinement by reducing grain size is hot rolling Multi-pass hot rolling is a preferred method for the materials that can show grain boundary recrystallization. Previous studies show that the main variable of hot rolling is the rolling temperature must be between 300℃ to 400℃ for magnesium alloys.

The high-pressure torsion (HPT) is a combined technique that includes two mechanical processes inside. A disk-shaped sample under high hydrostatic pressure between two anvils is exposed to torsional stress. After the high-pressure torsion (HPT) technique, the researchers achieved to produce sub micrometer or nanometer range grain sizes [41, 42]. The schematically illustration of the high-pressure torsion(HPT) is given in Fig. 2.10.

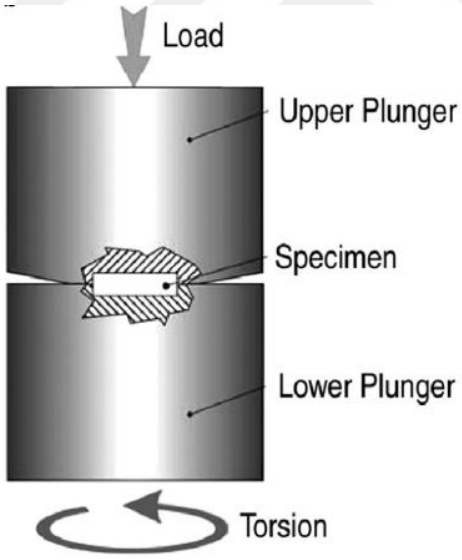

Figure 2.10 Schematic of high-pressure torsion (HPT) process [43].

Equal channel angular pressing (ECAP) method is using high shear stress for producing Ultra-Fine Grained (UFG) materials [44]. The microstructure of produced material by ECAP is in micro-scale grade. The ECAP is allowing the plastic deformation

with the same tubular section as unprocessed samples. ECAP process is shown in Fig.2.11. As shown in Fig. 2.11, different die angles affect the microstructure of the processed material.

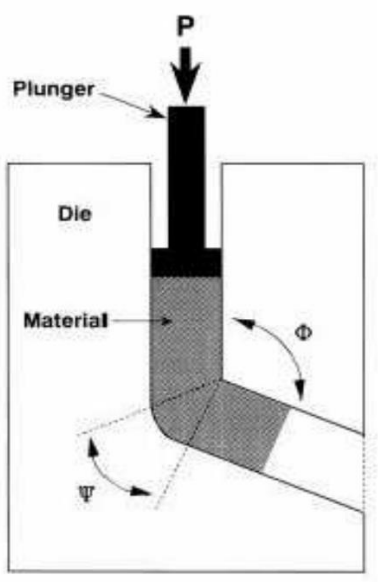

Figure 2.11 Schematic view of the equal channel angular pressing (ECAP) [45].

2.9 Rolling principles

Many works have been applied to the advancement of thermomechanical treatment processes for developing the mechanical properties of magnesium alloys to eliminate the formability limitation and spread the range of their applications [46, 47]. Warm rolling followed by post heat treatment is one of the most common methods for improving the mechanical properties of magnesium alloys. In the previous investigations, rolling was employed to enhance the strength of AZ magnesium alloys. For instance, Jeong et al. [48] observed a significant grain refinement of AZ31 after 50% warm rolling at 200°C, producing a grain size around 7 μm. Besides, they investigate the effect of warm rolling on the texture of AZ31 in detail. A traditional rolling process is shown in Fig. 2.12.

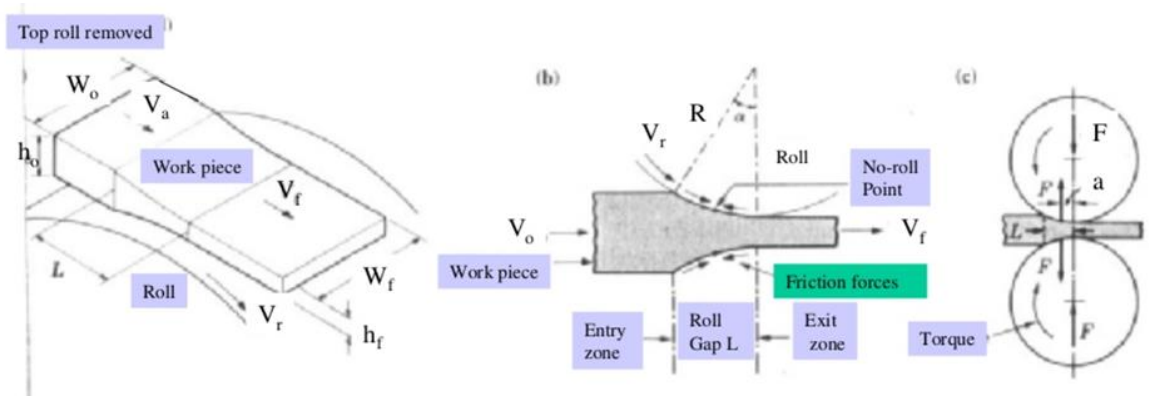

Figure 2.12 Schematic of the rolling process.

Considerable effort has been dedicated to the development of thermomechanical treatment processes for improving the mechanical properties of magnesium alloys to widen the range of their applications [7, 9]. One of the several methods for refining the mechanical properties of magnesium alloys is warm rolling. In the previous studies, warm rolling was used to improve the strength of the AZ31 magnesium alloy samples [11].

2.10 Precipitation Hardening

Precipitation hardening is a common heat treatment method that aimed to increase the yield strength of forgeable structural alloys of magnesium, aluminum, titanium, etc. Because of the age-hardening process, the solid-state precipitates are occurring. These alloys become stronger due to these precipitates [49]. The principle of precipitation hardening -also known as age hardening and particle hardening- is depending on the interaction between dislocations movements and occurred heat treatment particles. There are two different results of this interaction according to precipitate size. If the precipitate size is smaller than the critical value of dislocation, the result will be particle cutting. If the precipitate size is bigger than the critical value of dislocation, the result will be particle looping. Schematically illustration of particle cutting and particle looping are given in Fig. 2.13 and Fig. 2.14 [50].

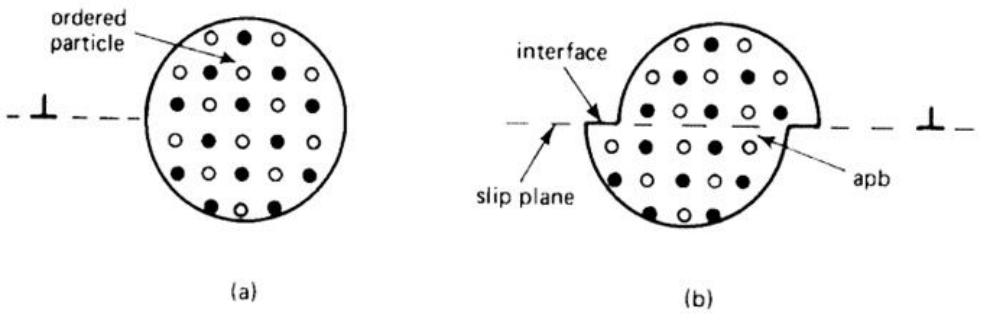

Figure 2.13 Ordered particles (a) cut by dislocations in (b) to produce new interface and apb [44].

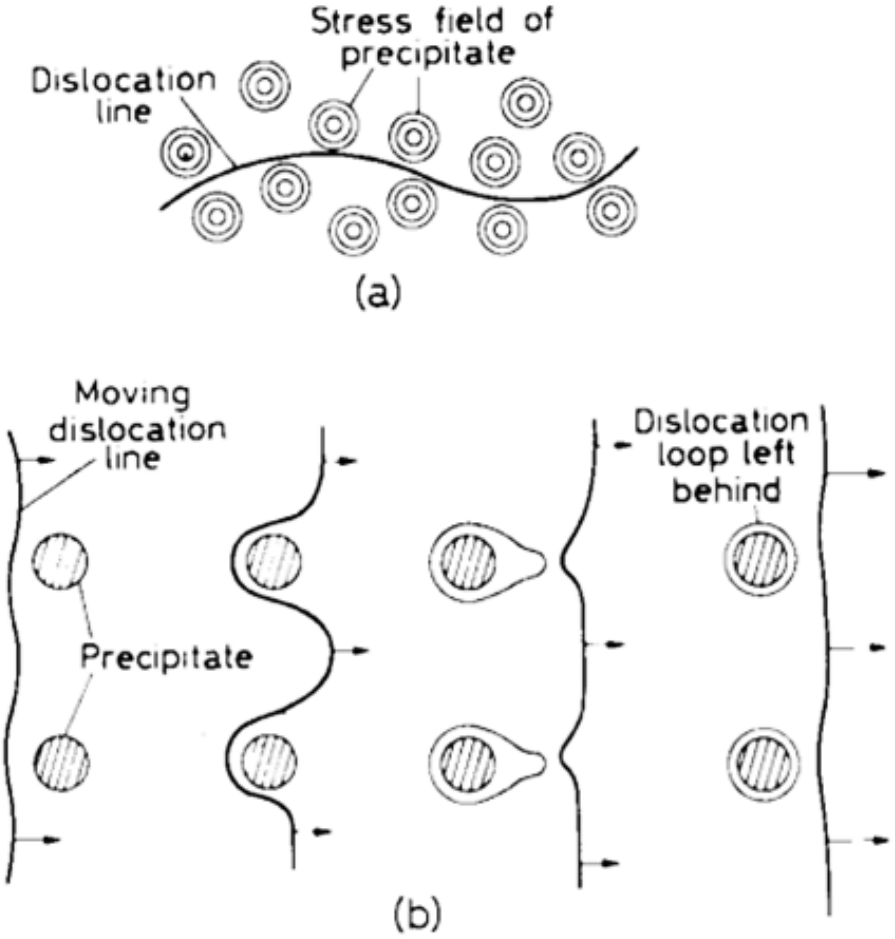

Figure 2.14 Schematic representation of a dislocation (a) curling round the stress fields from precipitates and (b) passing between widely spaced precipitates (Orowan looping and strengthening) [44].

Uematsu et al. [51] have examined the effect of aging on fatigue performance of AZ61 and AZ80. They detected β-phase $Mg_{17}Al_{12}$ precipitates near grain boundaries and within boundaries after aging at both conditions of T5 and T6. However, magnesium alloys do not have a suitable age-hardening response in comparison with aluminum alloys, due to the lower amount of precipitates. In spite of the previous researches about the warm rolling followed by age hardening of magnesium alloys, there is a lack of study concerning the influence of external stress during aging on the mechanical properties of AZ31.

2.11 Hall-Petch Strengthening

As mentioned previously, grain refinement processes are common and effective methods for the improve the strengthening of the materials. One of these grain refinement methods is Grain-boundary strengthening – also known as Hall–Petch strengthening- that enhance the strength of the material by changing the average grain size [52]. During the motion of the dislocations, grain boundaries behave as obstacles against dislocations movements.

$$\sigma_y = \sigma_0 + k_\sigma D^{-1/2} \quad (1)$$

The equation of Hall–Petch strengthening (1) is given as above. According to the equation, the yield stress (σ_y) is changing by the average grain size (D) because of the initial friction stress (σ_0) and the locking parameter (k_σ) are the constants. As determined by previous studies [53]. constant parameters for AZ31 magnesium alloy is given at below table.

Table 2.5 Constant parameters of Hall-Petch equation for AZ31 magnesium alloy [46].

Processing condition	Loading path	Grain Size (μm)	σ_o (MPa)	k_σ (MPa mm$^{1/2}$)
Rolling	Tension (in-plane)	16–40	60	10.5
Rolling	Tension //RD	5–25	45	10.1
Single rolling	Tension //RD	5–17	89	7.3
Rolling	Tension //RD	5–21	131	7.9
Rolling	Tension //RD	2–55	122	6.6
Rolling	Tension //RD	13–140	88	8.9
Rolling	Tension //TD	13–140	115	8.6
Extrusion and drawing	Tension //ED	3.5–12	120	5.0
Extrusion	Tension //ED	2.5–8	80	9.6
Extrusion	Compression //ED	3–11	22	12.3
FSP	Tension //AD	2.6–6.1	10	5.1
ECAP	Tension //ED	5–32	30	5.4
ECAP	Tension //ED	6–22	50	10.8
ECAP	Tension //ED	9–22	10	10.3
ECAP	Tension //ED	2–8	30	5.7

2.12 Thermal Conductivity of AZ31 magnesium alloy

Magnesium is widely researched for increase thermal conductivity by alloying it with materials that have higher thermal conductivity value than magnesium over the last few years. Especially mobile phone and computer industries are focused on magnesium alloys because of their low density and high thermal conductivity properties [54].

Thermal conductivity of the magnesium alloys can calculate with three variables that able to measure. The equation of the thermal conductivity is given at the below equation (2).

$$\lambda = \rho c p \alpha \qquad (2)$$

The thermal diffusivity (α: m2 · s−1) can measure by the commercial devices that use the laser flash method. The laser flash method uses an energy impulse that applied to the one side of the plane-parallel sample and calculates the time-based temperature rises on the other side of the sample [55].

The specific heat capacity (c_p: J · g−1 · K−1) measured by a differential scanning calorimeter. The third variable that needed to calculate thermal conductivity (λ) is the density (ρ: kg · m−3) that measures by Archimedes method [56].

3 EXPERIMENTAL PROCEDURES

3.1 As received material's characterization and preparation processes

In this study, AZ series magnesium alloy that commercial name AZ31 used as as-received material. Below Table 3.1 gives that the as-received AZ31 slab's chemical composition which analyzed with energy dispersive X-Ray (EDX) method.

Table 3.1 Chemical composition of AZ31.

Element	Al	Zn	Mn	Cu	Si	Fe	Mg
wt.%	3.23	2.43	0.79	0.77	0.16	0.11	Balance

The as-received AZ31 material was cut as the dimensions of 120×50×4 mm with electrical discharge machining (EDM) process. For the preparation of the as-received materials, an annealing treatment is applied to cut AZ31 slabs at 400°C for 3 hours. Vacuum furnace used for annealing with 10^{-3} mbar pressure to avoid the oxidation of AZ31 slabs during the annealing process. Also, the annealing process is needed to restore the formability and homogenize the microstructure of AZ31 slabs. After these steps, artificially applied static aging and stress aging process are allowing to occur uniform and fine precipitates.

3.2 Heat treatment

Magnesium alloys are very active alloys, and they react with the oxygen at high temperatures and even at ambient temperature. To prevent the oxidation of magnesium

alloys, all heat treatments such as annealing and aging treatments were performed on the samples using a furnace with a vacuum. The pressure of the furnace reduced to the 10^{-3} mbar and then heated up to the high temperatures for aging and annealing process. Fig. 3.1 shows the furnace and vacuum used in the current study.

Figure 3.1 vacuum furnace used for the heat treatment of magnesium alloy.

3.3 Warm rolling

The warm rolling process was applied to AZ31 samples for getting a stable structure that includes fine grains. 4 mm thick AZ31 slabs (3.23Al–2.43Zn–0.79Mn–Mg Bal. wt%) were utilized for the warm rolling process. As-received material with the annealed condition was homogenized at 400ºC for 3 h. A systematic warm rolling process was applied for the samples to reduce the thickness of plates to 1mm (75% of original thickness). The slabs were heated inside a furnace for 10 minutes at 300 °C and then rolled with 5% of the total reduction for each pass and quenched in water. The aforementioned method was repeated at every pass of unidirectional rolling. The rolling

speed of the rolling mill shown in Fig. 3.2 that was adjusted to 0.17 ms^{-1}. Additionally, to examine the effect of cross-rolling on the mechanical properties of AZ31 slabs cross-rolled with 90˚change in direction of rolling for each pass.

Figure 3.2 Rolling machine.

3.4 Stress aging process

Stress aging process was employed to AZ31 magnesium alloy samples to investigate the effect of the applied load on the samples during the aging process on the precipitation hardening and mechanical behavior of the samples. The stress aging apparatus is shown in Fig 3.3 was made to applied 50 MPa stress on the samples during the aging process. Also, the vacuum pump and chamber utilized to reduce the pressure of the air around the sample during the stress aging process. As mentioned before, the reduction of pressure prevents the oxidation of magnesium alloys at high temperature.

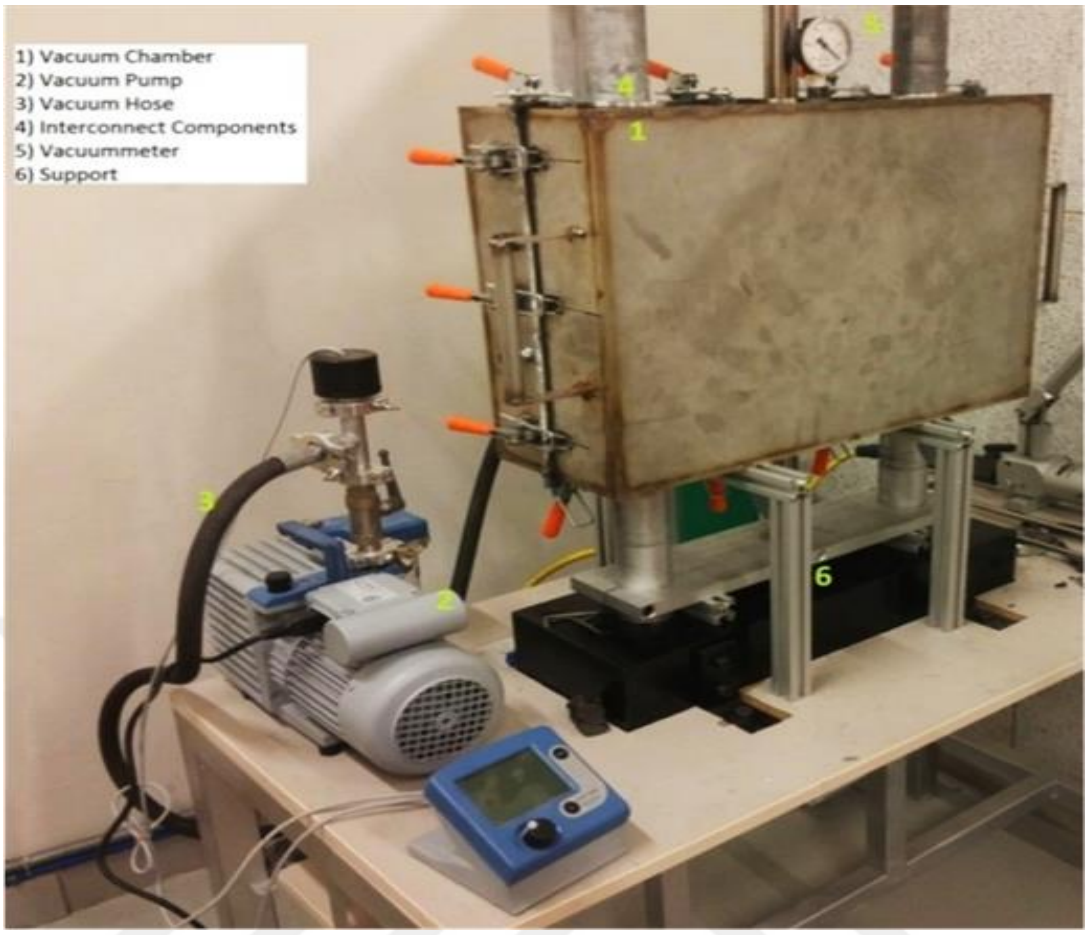

Figure 3.3 Stress aging apparatus with vacuum chamber.

Stress aging apparatus is assembled with several parts and devices that include a vacuum chamber, vacuum pump, load system, and heating system. The vacuum pump connected to the vacuum chamber to provide an environment to prevent oxidation. Load of the samples is controlled by a load cell that assembled to the central mill. Also, the sample grips are attached to the central mill. The sample is placed to the sample grips. The aging process was carried out under the pressure of 10^{-3} mbar inside of the stress aging apparatus to prevent the adverse effects of oxidation. The heating system ensures the requested value of the sample temperature with resistive heating. In this study, the load value determined as 50MPa. The duration of aging and the aging temperature values are given in Table 3.2.

Table 3.2 Stress aging conditions.

No	Condition	Aging temperature (°C)	Aging Duration (h)
1	75% warm rolled and stress aged under 50MPa	120	1
2	75% warm rolled and stress aged under 50MPa	120	3
3	75% warm rolled and stress aged under 50MPa	120	6
4	75% warm rolled and stress aged under 50MPa	120	12
5	75% warm rolled and stress aged under 50MPa	180	1
6	75% warm rolled and stress aged under 50MPa	180	3
7	75% warm rolled and stress aged under 50MPa	180	6
8	75% warm rolled and stress aged under 50MPa	180	12

3.5 Mechanical testing

3.5.1 Hardness measurement

ASTM standard for microhardness testing was used to prepare the samples. The Grinding process was carried out up to 2500grits then the specimens were mechanically polished employing the 6, 3 and 1µm diamond suspensions. Microhardness of the specimens after grinding and polishing was tested utilizing a Vickers indenter with a force of 1Kgf with a dwell time of 15s. At least, three tests were conducted on the samples of each condition to satisfy the accuracy and repeatability of the results. The mean value of the achieved results was used in the thesis and furthermore, the standard deviations of the results were smaller than 5%.

3.5.2 Uniaxial tensile tests

The bulk mechanical behavior of the thermo-mechanically processed AZ31 magnesium alloys was experimented using the uniaxial tensile tests. All the samples were

tested at ambient temperature under the strain rate of 0.001 s^{-1}. This strain rate was selected to satisfy the quasi-static condition of loading for the samples.

The ASTM standard was used for the preparation of the samples. Dog-bone shaped tensile specimens have been cut employing electro-discharge machining (EDM) with 15 mm gauge length. The samples were cut through the rolling direction. Furthermore, the samples were ground and mechanically polished to eliminate the influence of residual stresses and scratches form in the rolling and heat treatment process.

As shown in Fig. 3.4 a servo-hydraulic mechanical testing frame used to characterize the mechanical behavior of the samples at room temperature. Also, the elongation and consequently the strain of the specimens were measured utilizing an extensometer.

Finally, the mechanical tests samples were packed to prepare the fracture surface for further fracture morphology analysis.

Figure 3.4 A servo-hydraulic mechanical testing frame.

3.6 Microstructure evaluation methods

3.6.1 Optical microscopy observation

The samples were cut in small dimensions using the micro-cutting machine than were mounted using a hybrid of resin epoxy and hardener.

Standard metallographic preparation method was employed. The grinding process was performed with 500,800, 1200, 1500 and 2500 grits SiC papers. Water used as a lubricant during the grinding process to avoid increasing the temperature of the samples and prevent the destruction in the microstructure.

6, 3 and 1 μm cloths were employed for mechanical polishing by a diamond suspension. Throughout the polishing process, ethanol-based lubricant was used to avoid oxidation and surface scratching.

After that, the etching solution was provided for AZ31 magnesium alloys samples. The samples were chemically etched in a solution of 10 ml acetic acid, 5gr picric acid, 70 ml ethanol and 10 ml distilled water for the 30s to expose grain boundaries. An optical microscope was contracted to reveal the microstructure of the samples in low magnification of 20x and high magnification of 50x.

3.6.2 Scanning Electron Microscopy (SEM)

The fracture morphology of different conditions of as-received, rolled, aged, and stress aged AZ31 magnesium alloys were observed using scanning electron microscopy (SEM). As shown in Fig. 3.5, a ZEISS SEM at an accelerating voltage of 15kV was utilized for this work.

Figure 3.5 ZEISS scanning electron microscope (SEM).

Before conducting the SEM observations, the physical vapor deposition (PVD) were applied for covering the surface of the AZ31 magnesium alloys with palladium (Figure 3.6). The coating was done using the argon gas in the condition of 4×10^{-2} mbar and a duration of 2 minutes to enhance the conductivity of the samples and quality of SEM images.

Figure 3.6 PVD coating machine.

3.7 Thermal conductivity measurement

The thermal conductivity of different conditions of as-received, aged, and stress aged AZ31 magnesium alloys were observed with thermal diffusivity measurement device which using laser flash analysis method (LFA). The thermal diffusivity measurement device (Figure 3.7) uses an energy impulse that applied to the AZ31 magnesium disc-shaped samples and calculates the time-based temperature rises of the samples. Because of the technical specifications of the thermal diffusivity measurement device, AZ31 samples were cut as the diameter of 12.6 ± 0.1 mm with EDM.

Figure 3.7 The thermal diffusivity measurement device.

The specific heat capacity (c_p) measured by a commercial differential scanning calorimeter device. The third variable that needed to calculate thermal conductivity (λ) is the density (ρ) that measured by the equation of density ($\rho = mV^{-1}$).

4 RESULTS AND DISCUSSION

4.1 Microstructure and microhardness observations

As shown in Fig. 4.1, after 75% warm rolling coarse grain structure of as-received AZ31 was refined significantly. Fig. 4.1a displays grain size variation from 6 to 67 μm with an average size of 48μm. The density of dislocations and grain boundaries were increased and subsequently its improved the strength of the rolled samples [57]. The average grain size of the as-received AZ31 was about 48μm and after the warm rolling process, the mean grain size was reduced near to the 8μm.

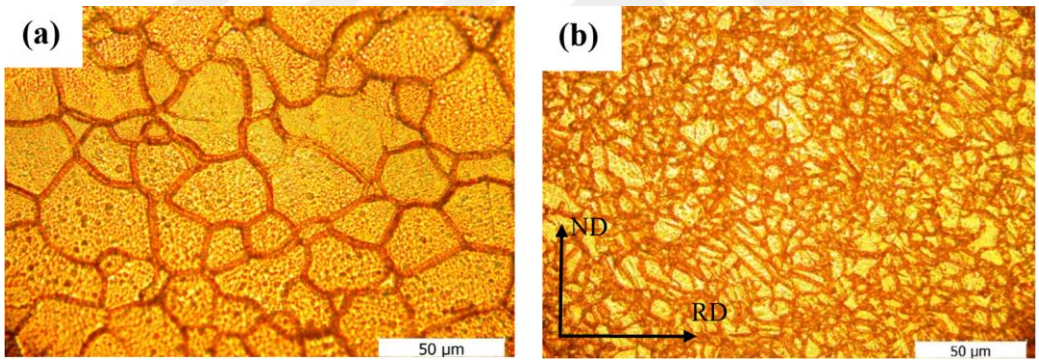

Figure 4.1 OM of AZ31 for (a) as-received and (b) 75% warm rolled conditions.

As it was mentioned in the previous section, the aging process was applied on the rolled samples at different temperature of 120 ˚C and 180 ˚C for various durations ranging from 1h to 48h. Fig. 4.2 demonstrates the optical metallographic microstructure of the rolled AZ31 magnesium alloys after conventional aging at 120 ˚C. After 1h aging still, the grain size was very fine and grain growth was not observed in the microstructure of the sample (Fig. 4.1b and Fig. 4.2a).

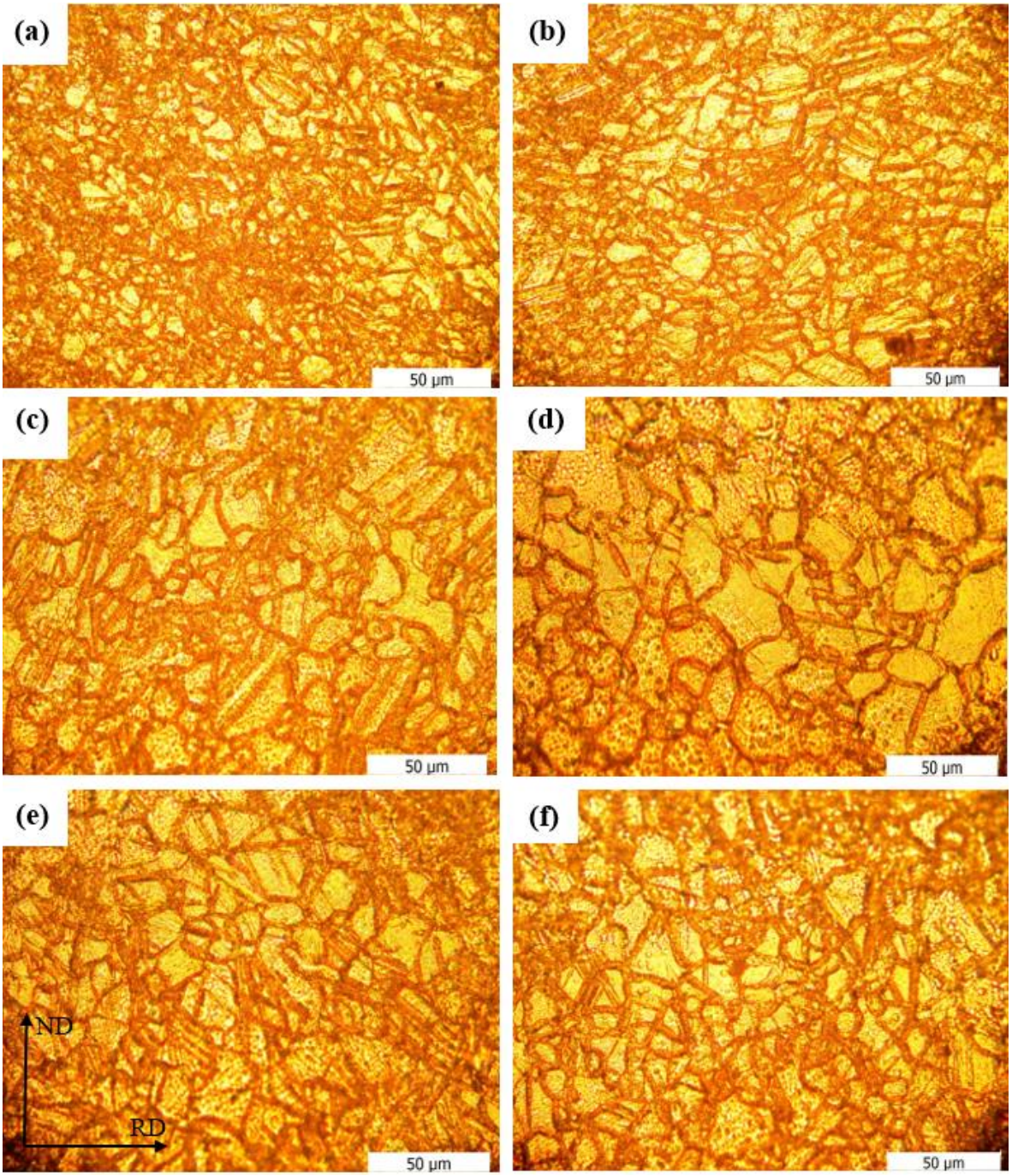

Figure 4.2 OM of AZ31 after 75% warm rolling and aging at 120˚C for (a)1h, (b)3h, (c)6h, (d)12h, (e)24h, and (f)48h.

The microstructural variations happening throughout the aging of the warm rolled AZ31 magnesium alloy lead to the reduction of the stored energy due to high plastic deformation. For the samples after 3h and 6h aging at 120 ˚C, grain growth of the fine

grains is obvious and the average grain size of the samples was increased up to about 15μm (Fig. 4.2b and c). As shown in Fig. 4.2d after 12h aging at 120 ˚C, despite the initially fine grains produced in the rolling process, were grown during the aging process, the recrystallized new grains started to nucleate. An inhomogeneous structure includes the coarse grains and recrystallized grains were discovered in OM micrograph.

With increasing the duration of the aging process up to 24h and 48 h, the recrystallized grains were grown and the microstructure of the samples was started to be more homogeneous (Fig. 4.2e and f). The same aging process was applied to the samples at 180 ˚C for the different aging time of 6, 12, 24, and 48h. Fig. 4.3 illustrates the grain growth and recrystallization of new grains in the microstructure of AZ31 magnesium alloy. On the contrary, the recrystallization phenomenon for aging at 180 ˚C was started sooner, after 6h (Fig. 4.3a). Similarly, grain growth and homogenization of recrystallized grains occurred (Fig. 4.3c and d). During the aging process at 180 ˚C, the average grain size of the samples firstly increased from 8μm up to 24μm and then decreased to about 17μm after 48h aging.

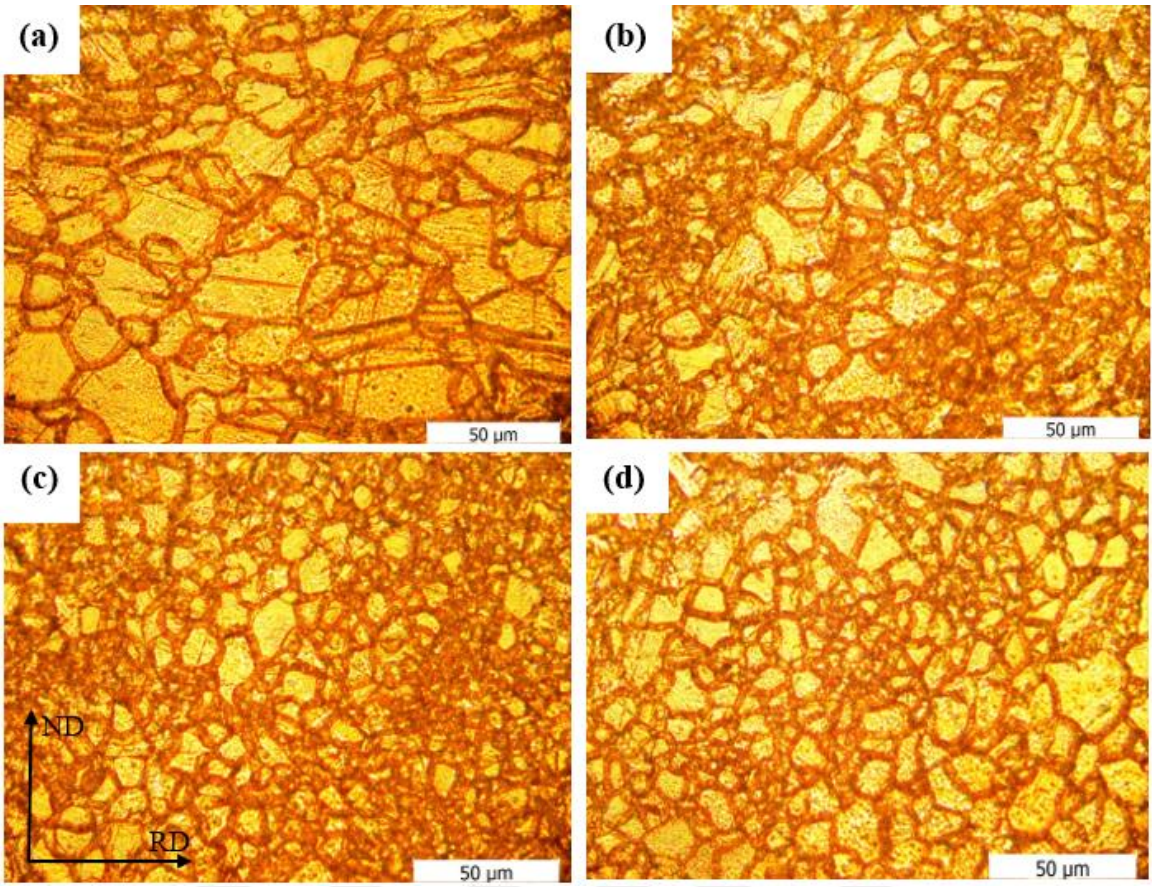

Figure 4.3 OM of AZ31 after 75% warm rolling and aging at 180˚C for (a)6h, (b)12h, (c)24h, and (d)48h.

On the other hand, the microstructure evolution of AZ31 for the different conditions of rolled plus stress aging is shown in Fig. 4.4 and Fig. 4.5. AS shown in Fig. 4.4, nucleation of recrystallized grains was initiated after only 1h stress aging under the stress level of 50MPa at the temperature of 120 °C. Nucleation of recrystallized grains was very faster than the conventional aging due to the powerful support of stress aging on the precipitation hardening of AZ31 [58].

The effect of Orowan strengthening on the tensile behavior of the AZ series of magnesium alloys due to the nanoscale precipitate of β-$Mg_{17}Al_{12}$ phases was investigated previously [59, 60]. The precipitation hardening for magnesium alloys arises from an

aging treatment for a supersaturated solid solution at a temperature range of 100–300 °C [59].

The stress aging temperatures for this study were selected as 120 °C and 180 °C. Furthermore, the presence of precipitates provides an opportunity to accelerate the nucleation due to particle-stimulated nucleation (PSN).

The influence of large particles in advancing recrystallization by the mechanism of particle-stimulated nucleation is properly known and widely observed [30]. The occurrence of PSN in magnesium alloys is very often and it's reported by various researchers [61-63], although the direct evidence was not convinced to date. PSN has been considered in greatest detail for aluminum alloys. The method is accelerated sub-boundary migration in the deformation region which fundamentally shapes nearby the large and hard particles throughout deformation, attending to the production of new high-angle grain boundaries (HAGBs) [64].

The yield strength of stress aged sample at 120 °C for 1 h remained at about 240 MPa attributed to the particle-stimulated nucleation and also the pinning effect of precipitates, which prevent the grain growth of recrystallized grains [65, 66].

Also, the average grain size of the sample stress aged at 120C was about 14μm and after 12h stress aging process the average size did not increase significantly, where the grain size of 12h stress aged sample was around 17μm. This stability of grains is attributed to the pinning effect of the β-$Mg_{17}Al_{12}$ phases distributed in AZ31 magnesium alloy [59].

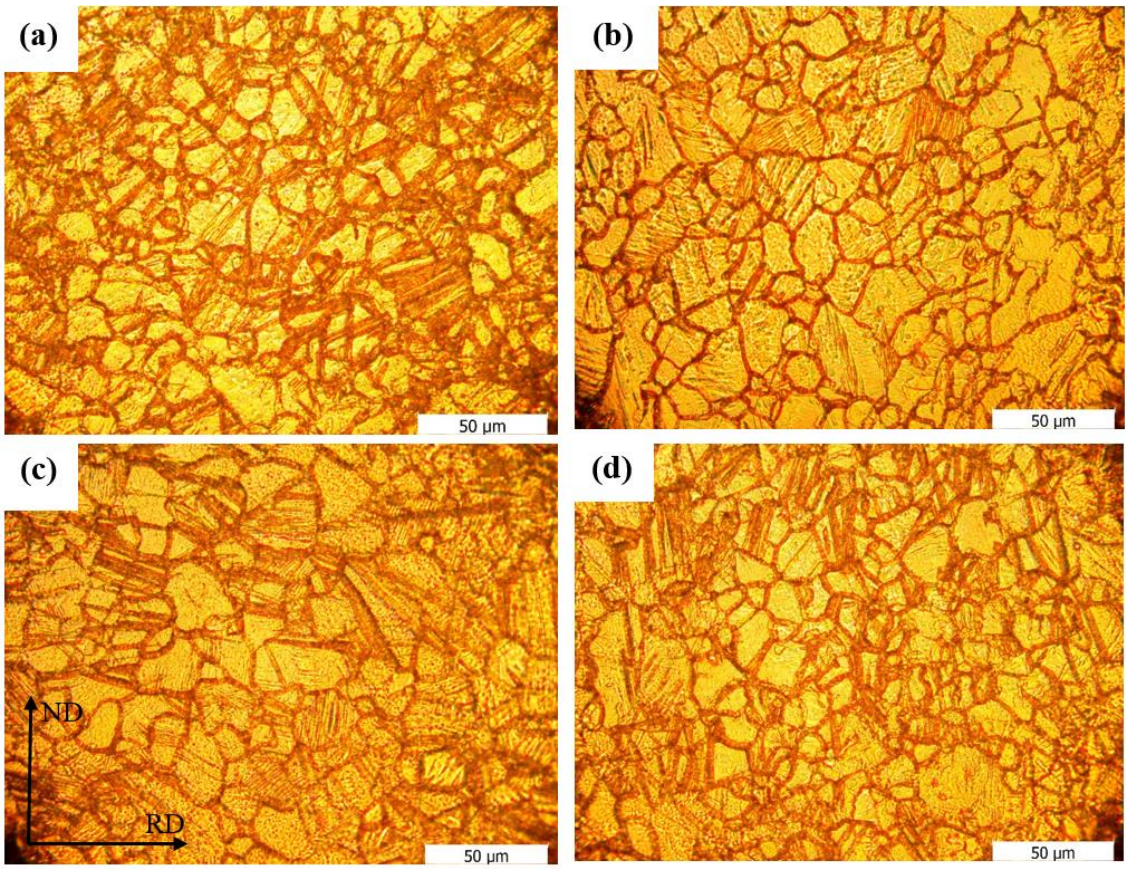

Figure 4.4 OM of AZ31 after 75% warm rolling and stress aging under 50MPa at 120˚C for (a)1h, (b)3h, (c)6h, and (d)12h.

On the other hand, for the samples, stress aged under the stress level of 50MPa at the temperature of 180C, it can be seen that although the recrystallization happened quickly, the grain growth of the recrystallized grains also occurred and its reduced the strength of the samples after the aging process (Fig. 4.5). Also, variety of grain size after stress aging is obvious in Fig. 4.5b-d and the average grain size of the samples increased from 19µm for 1h stress aged sample up to about 28µm after 12h stress aging.

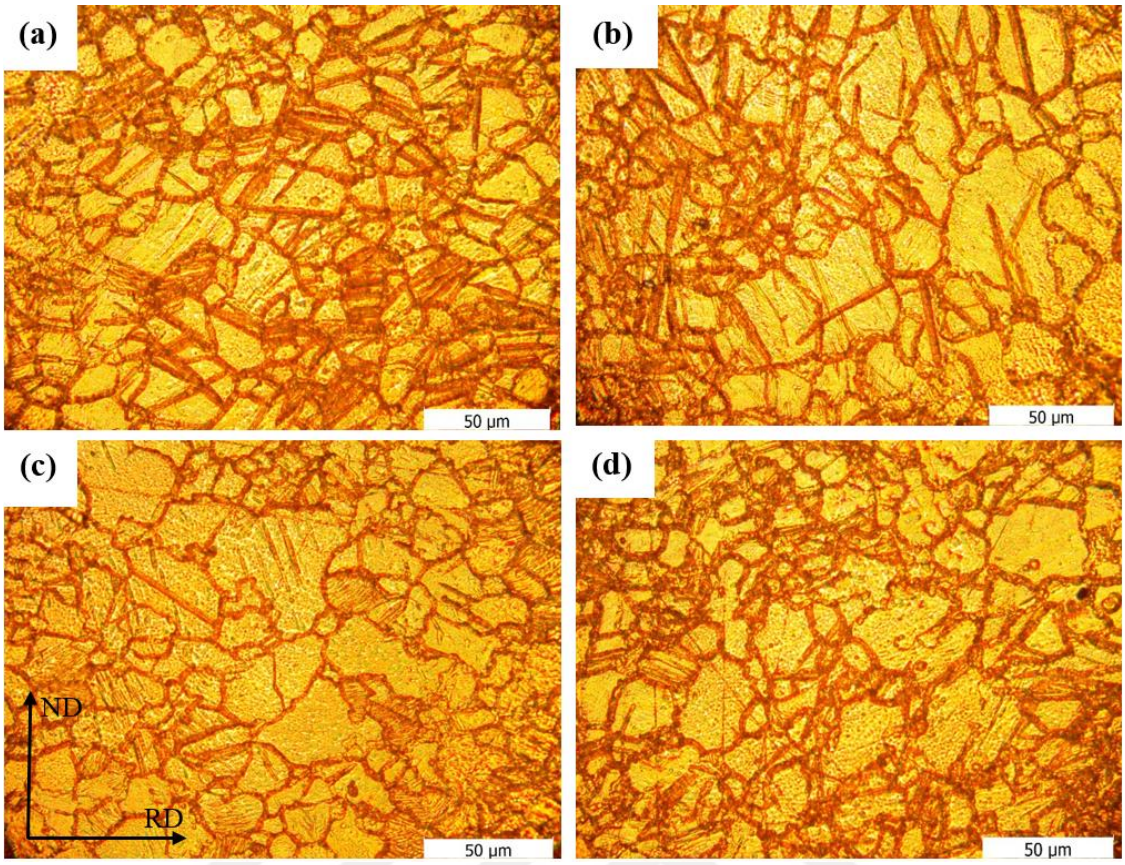

Figure 4.5 OM of AZ31 after 75% warm rolling and stress aging under 50MPa at 180˚C for (a)1h, (b)3h, (c)6h, and (d)12h.

4.2 Mechanical properties

The uniaxial tensile test has been conducted on the samples to characterize the tensile behavior of them after warm rolling and different heat treatments. Fig. 4.6 demonstrates the effect of warm rolling on the as-received AZ31 magnesium alloy. The rolling process improved the yield point of the sample from 166MPa to about 250MPa due to increasing the dislocation density and grain boundary density after 75% rolling while the ductility was decreased to around 6%. Also, the ultimate tensile strength (UTS) was increased up to 291MPa after the rolling process. Although, the yield and ultimate strength of the sample were enhanced after the rolling, the reduction of ductility limits the application of the materials. Then further thermomechanical processing is necessary to

improve the ductility of the sample with saving the high strength achieved from the rolling process.

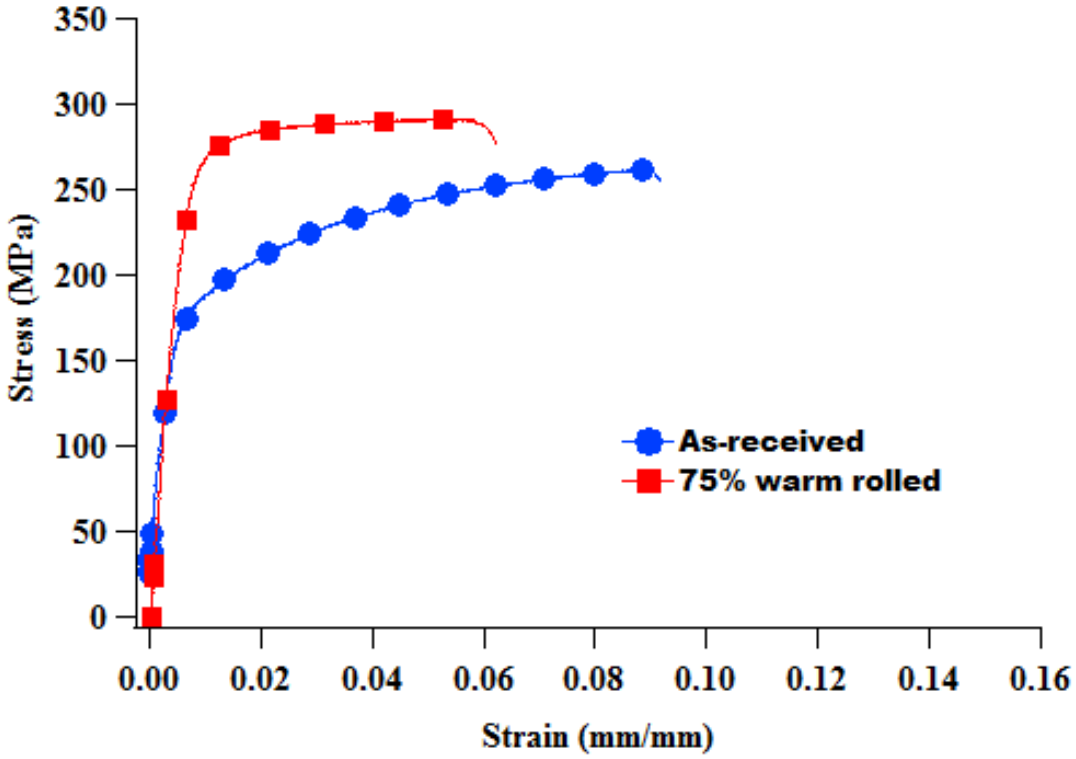

Figure 4.6 Stress-strain curves of AZ31 for as-received and 75% warm rolled conditions.

Fig. 4.7 represents the stress-strain curves of conventionally aged samples after the rolling process. Inspection of data from Fig. 4.7a revealed that aging at 120˚C after 6h has recovered the lost ductility of the rolled alloy and strain at failure increased to 9% which is equal to the as-received condition. But this improvement of ductility was accompanied by a reduction of yield and ultimate strength of the sample. Furthermore, increasing the aging time up to 48h the strain at failure was increased to 13% due to the grain growth of the newly recrystallized grains.

As shown in Fig. 4.7a, noticeable reduction in the yield strength of the sample aged at 120 ˚C after 12h was observed which is attributed to the high grain growth level of AZ31, detected in the microstructure of sample (Fig 4.2d). After that with increasing the duration of aging at 120˚C nucleation of newly recrystallized grains enhanced the strength of the samples for 24h and 48h aging durations. Another contribution to this improvement in strength can be attributed to the Orowan strengthening of nanoscale precipitate of β-Mg17Al12 phases produced throughout the aging process [60]. It should be noted for this reasoning, the strengthening due to precipitates should not vary significantly for the aforementioned aging durations.

Additionally, Fig. 4.7b illustrates a better ductility for the samples aged at the temperature of 180˚C with the expense of a significant decrease in strength of the rolled sample. The aforementioned, phenomenon is related to the acceleration of grain growth of the fine grains throughout the aging process at 180˚C.

Also, it can be seen that the effect of aging duration at 180 ˚C was relatively negligible compared with the samples aged at 120 ˚C due to the over aging the samples at 180 ˚C. The results of the tensile tests were in a good agreement with the optical microscopy observation, explained in the previous section.

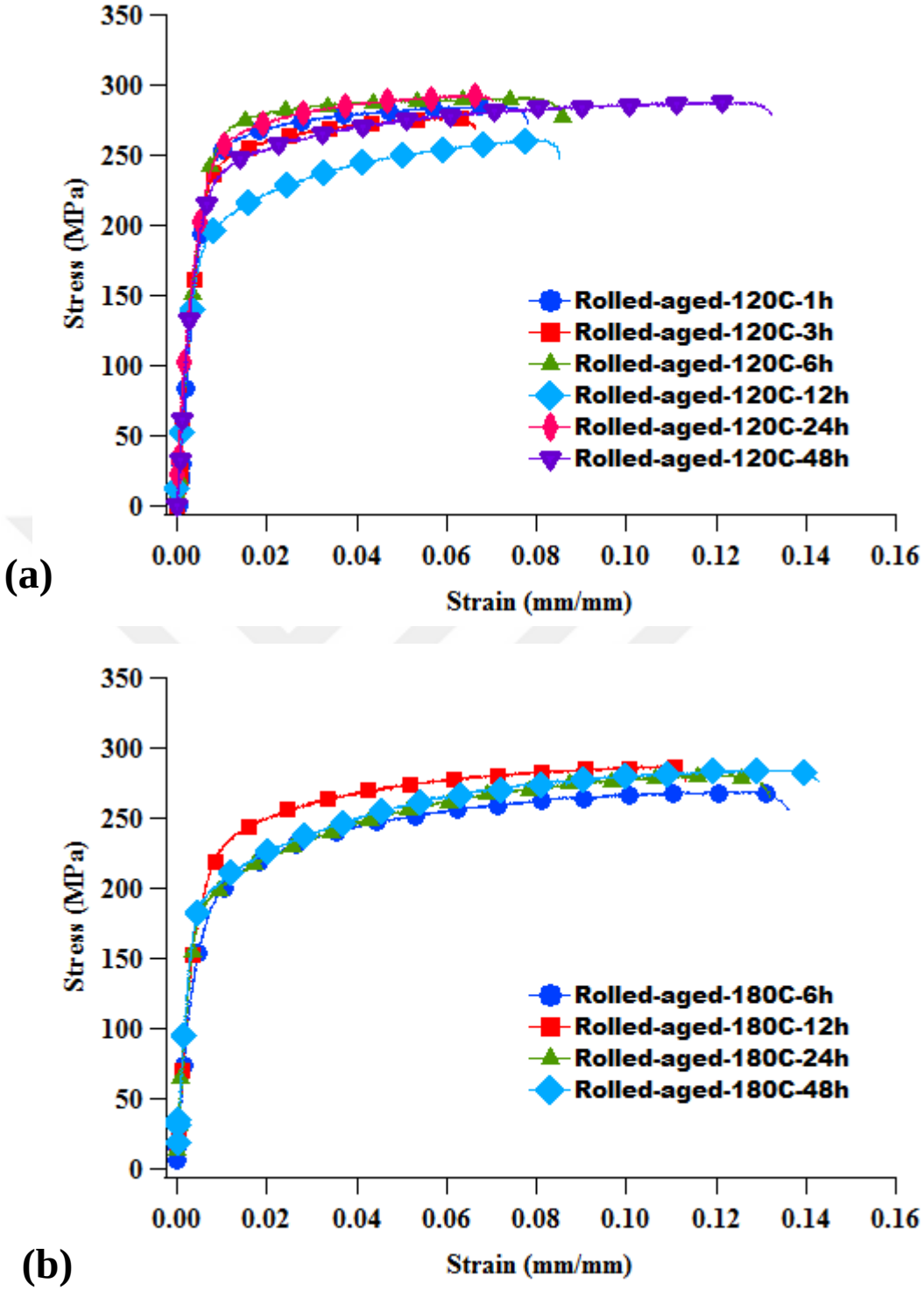

Figure 4.7 Stress-strain curves of 75% warm rolled AZ31 after different aging temperature of (a) 120˚C and (b) 180˚C.

Fig. 4.8 demonstrates the effect of stress aging on the stress-strain curves of the AZ31 magnesium alloy at a different aging temperature of 120˚C and 180˚C under the

stress level of 50MPa. AS shown in Fig. 4.8a, the results of tensile tests revealed that stress aging at 120˚C for 1h increase the ductility of rolled samples without any reduction in yield strength due to the accelerated recrystallization of new grains and additionally the pinning effect of the formed β-$Mg_{17}Al_{12}$ phases during the stress aging [62].

Furthermore, the shape of the stress-strain curve of stress aged sample at 120˚C, after the yield point at the plastic zone manifested an approximately linear and mild slope which represents low strain hardening of the sample after 1h stress aging [67]. With increasing the duration of stress aging the ductility of the samples improved with the expense of the reduction in the yield strength, however, the UTS remained approximately constant due to the work hardening of the samples throughout the tensile test (Fig.4.8a).

On the other hand, for the samples stress aged at the temperature of 180˚C, although the UTS of the samples was nearly the same as the stress aged samples at 120˚C, the yield strength of them was decreased significantly. Aforementioned behavior was attributed to the grain growth of the samples at stress aging at 180˚C.

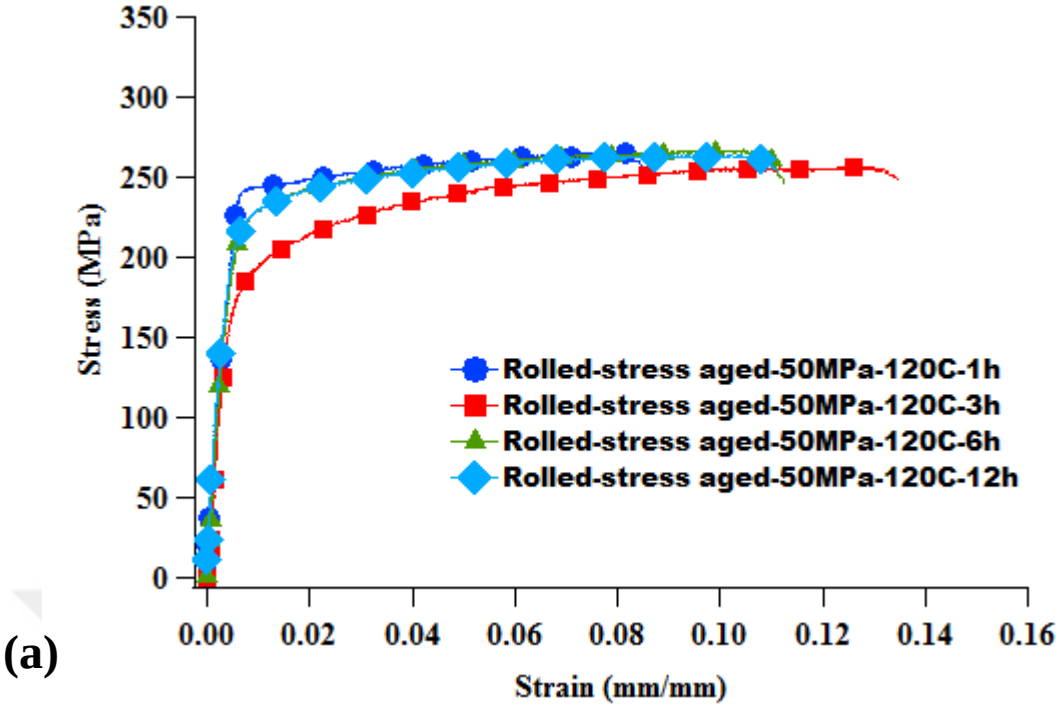

Figure 4.8 Stress-strain curves of 75% warm rolled AZ31 after stress aging under 50MPa at different temperature of (a) 120˚C and (b) 180˚C.

The tensile behavior of AZ31 after the different thermomechanical processing conditions are displayed in Fig. 4.9. Despite the low yield strength of as-received

condition (160 MPa) due to the coarse grains generated in annealing treatment and homogenization, the ultimate tensile strength reached to about 250 MPa attributed to the high strain hardening of annealed AZ31. Whereas the ductility of the as-received sample was limited to 8% due to the restricted slip systems of AZ31 with the hcp crystal structure. According to Fig. 4.9, the yield and ultimate strength of the as-received sample were enhanced up to 260 MPa and 292 MPa after 75% warm rolling with the expense of 3% reduction in ductility.

Further heat treatments were conducted on the rolled samples to recover the ductility. The stress-strain curves indicated that after 24 h aging at 120 °C the yield strength of the sample was decreased while the UTS and the maximum strain were enhanced a little. But for the sample which was aged at 120 °C for 48 h, the ductility improved up to 13% with the expense of a reduction in yield strength and approximately same UTS. The similar behavior was observed after aging at 180 °C for 48 h but the reduction of yield strength was more significant due to the grain growth of refined rolled microstructure after aging at 180 °C.

Also, the tensile behavior of stress aged sample under the stress level of 50 MPa at 120 °C for 1h is presented in Fig. 4.9. Comparison of the stress-strain curve of the stress aged sample with the others revealed that the strain hardening capacity of the rolled sample after stress aging was not recovered as much as the conventional aging process. Additionally, the yield strength of stress aged sample reached up to 240 MPa which is 50% higher than that of the as-received sample with nearly the same ductility. Stress aging provides decent strength levels with a much shorter aging period.

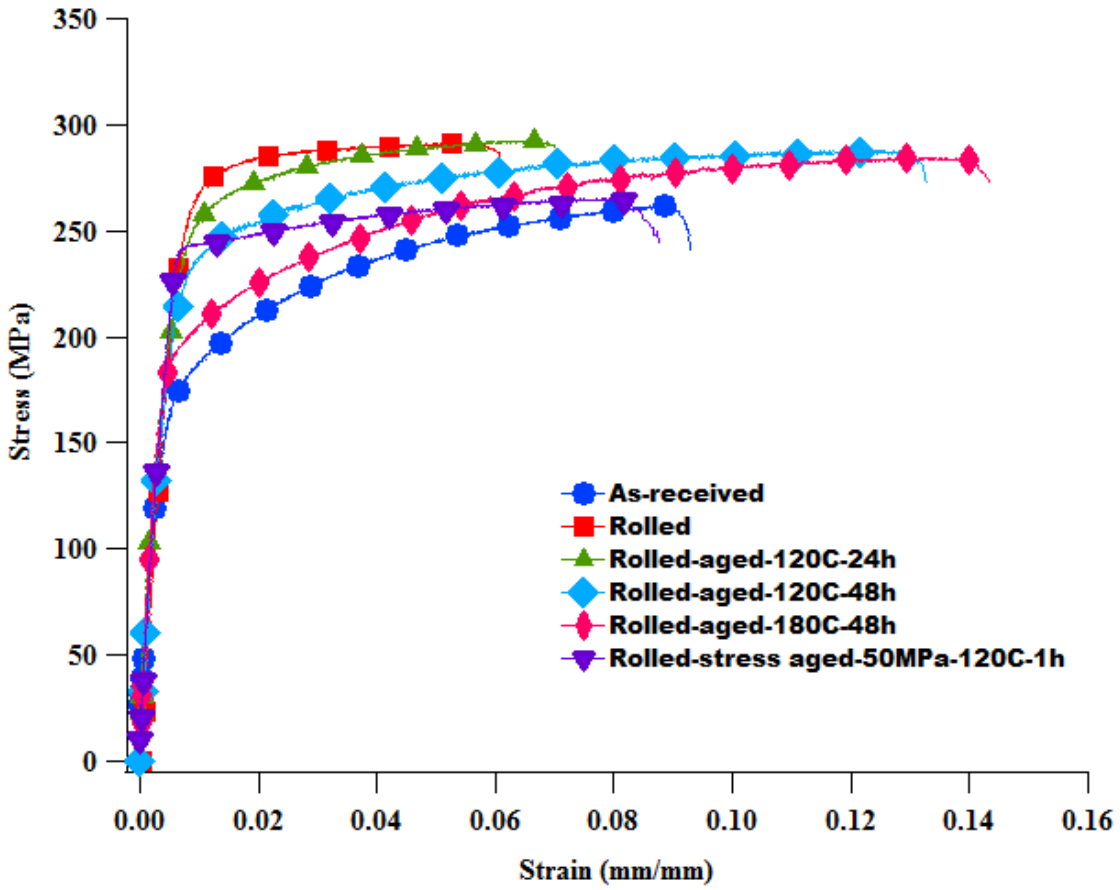

Figure 4.9 Stress-strain curves of AZ31 for different conditions.

Mechanical properties include yield and ultimate strength ductility and microhardness results as well as the average grain size for all condition of as-received, rolled, aged, and stress aged are listed in Table 4.1. The standard deviations of the mean value of the achieved results listed in Table 4.1 were smaller than 5%. Moreover, the toughness values for all conditions were calculated from the stress-strain curves and written in Table 4.1. Accordingly, the highest toughness is achieved in the sample stress aged at 120 °C for 3h.

Table 4.1 Hardness and tensile test results of AZ31 for different conditions.

Condition				Yield strength (MPa)	Ultimate strength (MPa)	Elongation at failure (%)	Hardness (Hv)	Average grain size (µm)	Toughness (J/mm^3)
As-received-homogenized at 400˚C for 3 h				166	267	9	47	45	21.0166
75% warm rolled				249	291	6	67	8	16.6791
	Conventional aged	120 ˚C	1 h	239	286	8	66	12	20.6116
			3 h	222	278	8	64	15	16.8841
			6 h	243	291	8	67	15	23.3744
			12h	185	261	8	59	18	19.8284
			24h	238	299	7	64	16	18.9071
			48h	215	288	13	61	24	35.4407
		180 ˚C	6 h	168	269	13	55	18	33.3597
			12h	197	287	11	63	22	29.7761
			24h	190	281	13	59	24	33.2224
			48h	192	285	14	62	17	36.7774
	Stress aged 50 MPa	120 ˚C	1 h	241	265	9	72	14	24.0407
			3 h	177	257	13	63	19	37.8136
			6 h	209	267	11	65	17	31.7105
			12h	212	264	11	58	18	21.3857
		180 ˚C	1 h	199	258	10	51	19	19.3205
			3 h	189	263	14	53	24	32.2187
			6 h	173	250	13	57	25	29.2513
			12h	179	246	9	55	28	22.2154

4.3 Cross-rolling

In order to observe the effect of rolling direction and the difference between the mechanical properties of unidirectional rolling and cross-rolled AZ31 magnesium alloys, microstructural evolution and tensile properties of 50% cross-rolled samples were investigated.

As shown in Fig. 4.10, approximately homogenized coarse grains of solution treated as-received AZ31 were relatively refined after 50% cross-rolling. Although the grain refinement was observed after the cross-rolling process, the grain growth inside of the microstructure of the sample was detected attributed to the heating before each rolling pass for 10 minutes at 300°C. Moreover, the existence of twins entire the all samples after cross-rolling is obvious and more pronounced as compared to uni-directional rolling sample (Fig. 4.10b).

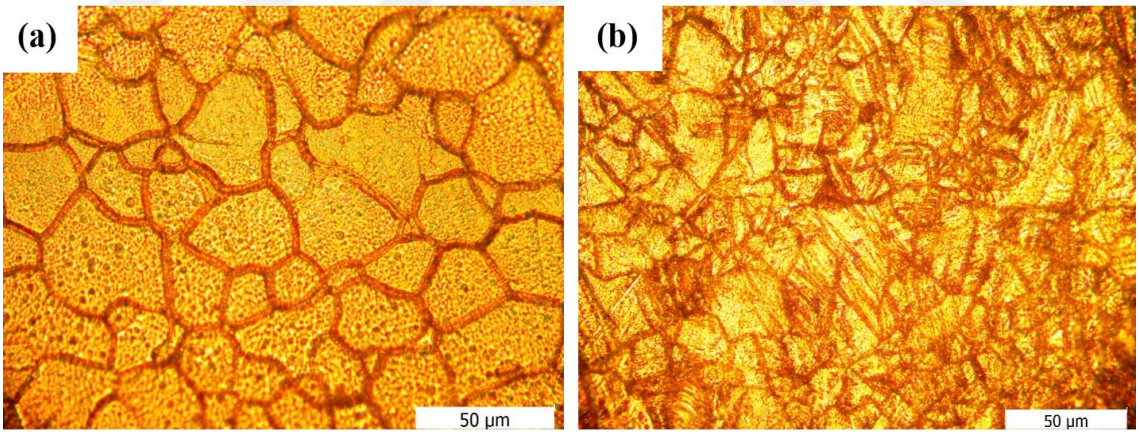

Figure 4.10 OM of (a) AZ31 as-received and (b) after 50% warm cross-rolling.

The microstructural evolution during the conventional aging at 120˚C and 180˚C after the cross-rolling process is demonstrated in Fig. 4.11. After 12h conventional aging at 120˚C, recrystallized new grains were formed in the sample and then a stable microstructure was detected for 48h duration (Fig 4.11a and b). On the other hand, the

microstructure of samples aged at 180˚C represents relatively coarse grains mixed with fine recrystallized new grains due to the moderately high aging temperature of 180˚C which may cause to the grain growth. Comparing the microstructure of samples aged at 120˚C and 180˚C, it can be detected that the microstructure of treated samples at 120˚C are finer than the samples treated at 180˚C (Fig. 4.11).

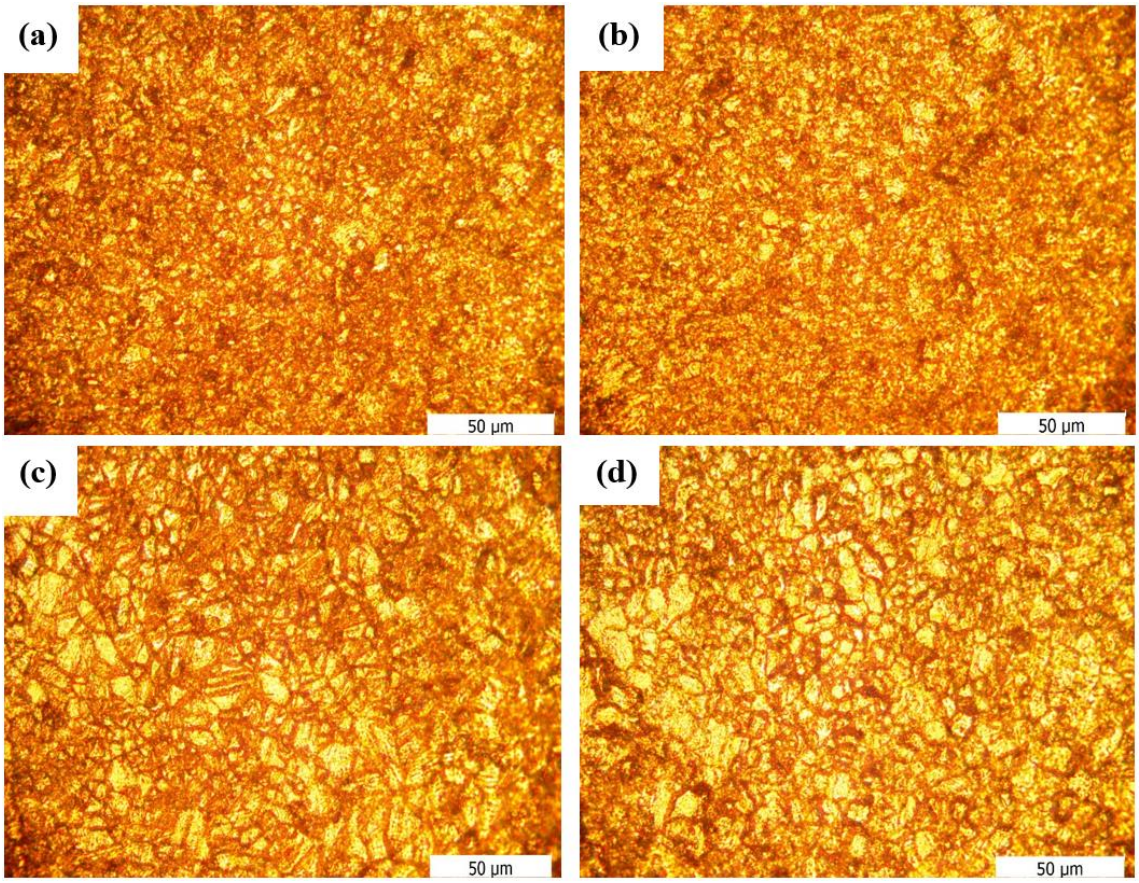

Figure 4.11 OM of AZ31 after 50% warm cross-rolling and conventional aging at (a)120˚C for 12h, (b) 120˚C for 48h, (c) 180˚C for 12h, and (d) 180˚C for 48h.

The effect of stress aging on the microstructure of warm cross-rolled samples for the different aging temperature of 120˚C and 180˚C under the stress level of 50MPa with duration raging from 1h to 12h is illustrated in Fig.4.12 and 4.13, respectively. A stable microstructure during the stress aging was detected for different durations at 120˚C. The

construction of twins in the microstructure of AZ31 magnesium alloy is obvious in the figures during the stress aging (Fig. 4.12b and c).

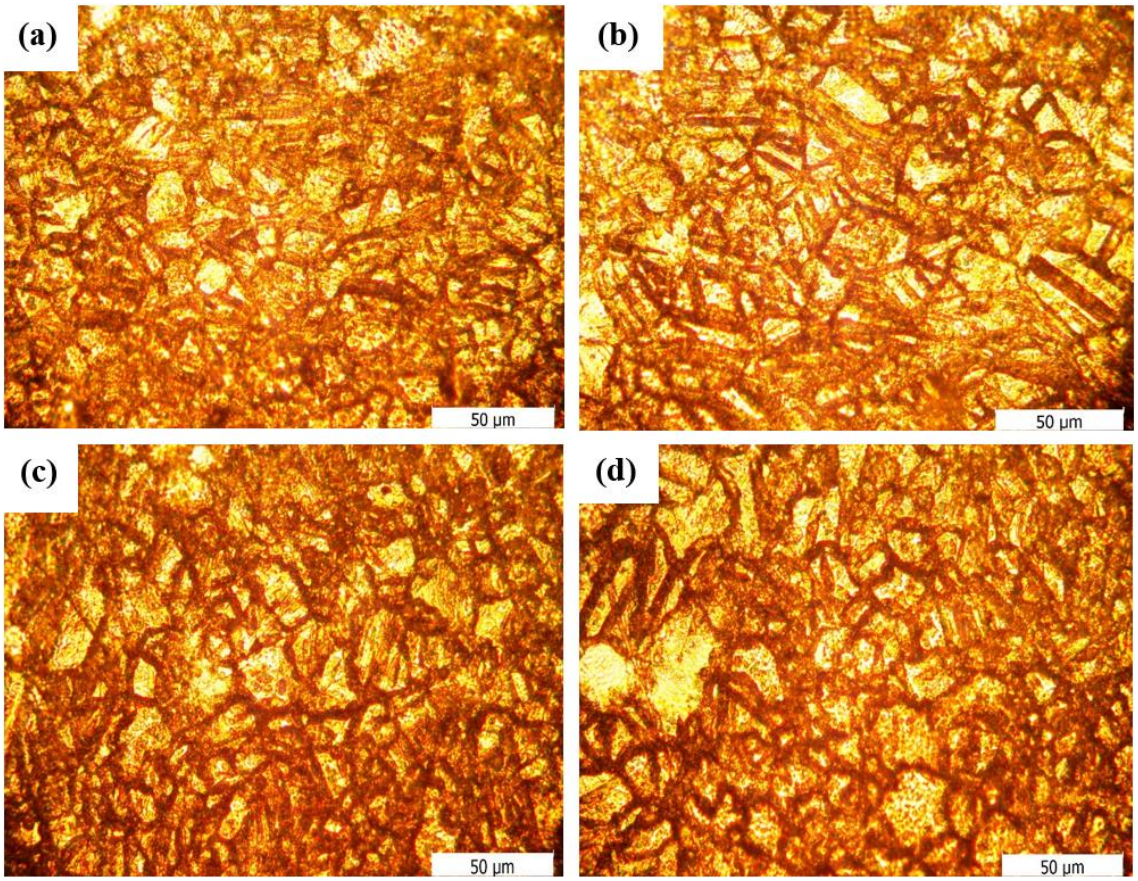

Figure 4.12 OM of AZ31 after 50% warm cross-rolling and stress aging under 50MPa at 120˚C for (a)1h, (b)3h, (c)6h, and (d)12h.

Additionally, the grain growth of the newly recrystallized grains is more clear for the samples stress aged at 180˚C due to the high temperature of aging that accelerating grain growth of the samples (Fig. 4.13). Also, mixed microstructures containing fine and coarse grains were observed in all conditions of stress aging at 180˚C.

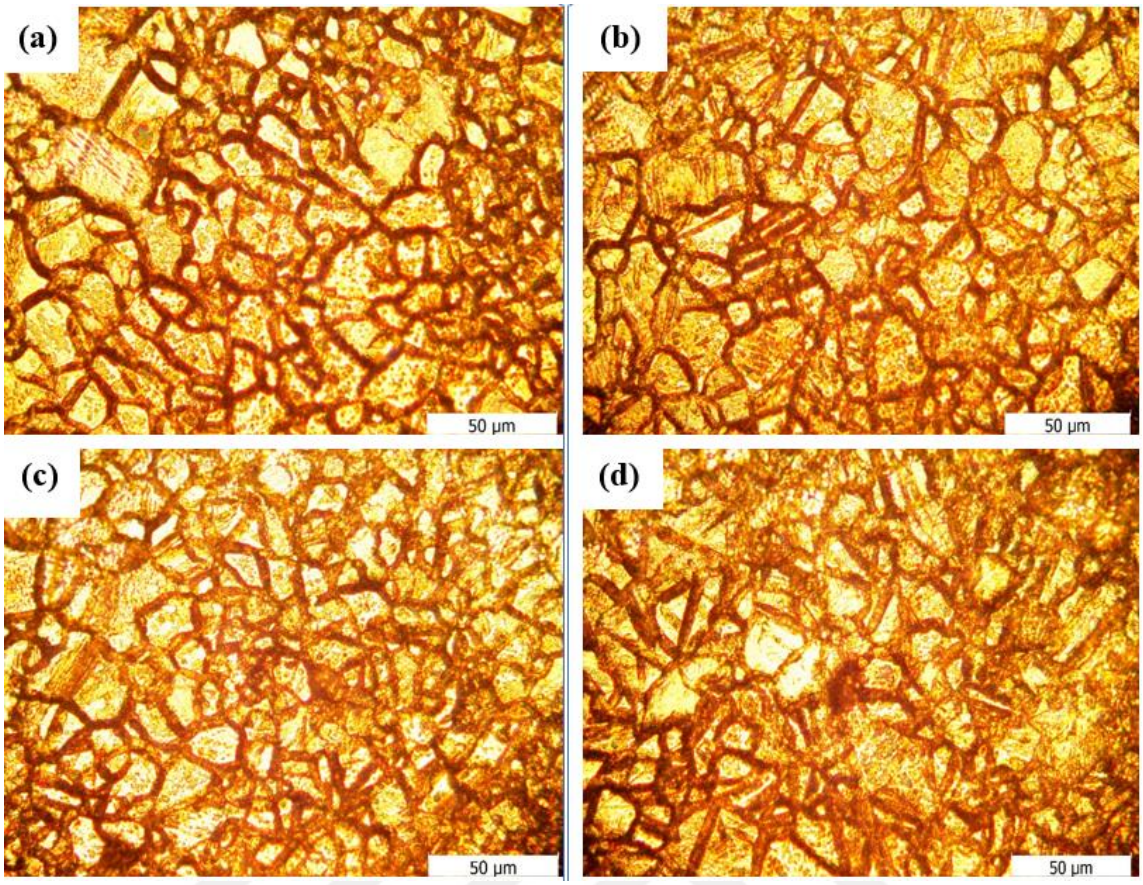

Figure 4.13 OM of AZ31 after 50% warm cross-rolling and stress aging under 50MPa at 180˚C for (a)1h, (b)3h, (c)6h, and (d)12h.

Fig. 4.14 shows the tensile behavior of cross-rolled samples after various conditions of conventional and stress aging. Inspection of data obtained from the stress-strain curves revealed that warm cross-rolling of as-received AZ31 was not effective to improve the strength of the sample and slightly only the ductility of the as-received sample was increased after cross-rolling. This can be attributed to the repeated heating process before each pass of rolling associated with multiple changes of rolling direction throughout the cross-rolling [57].

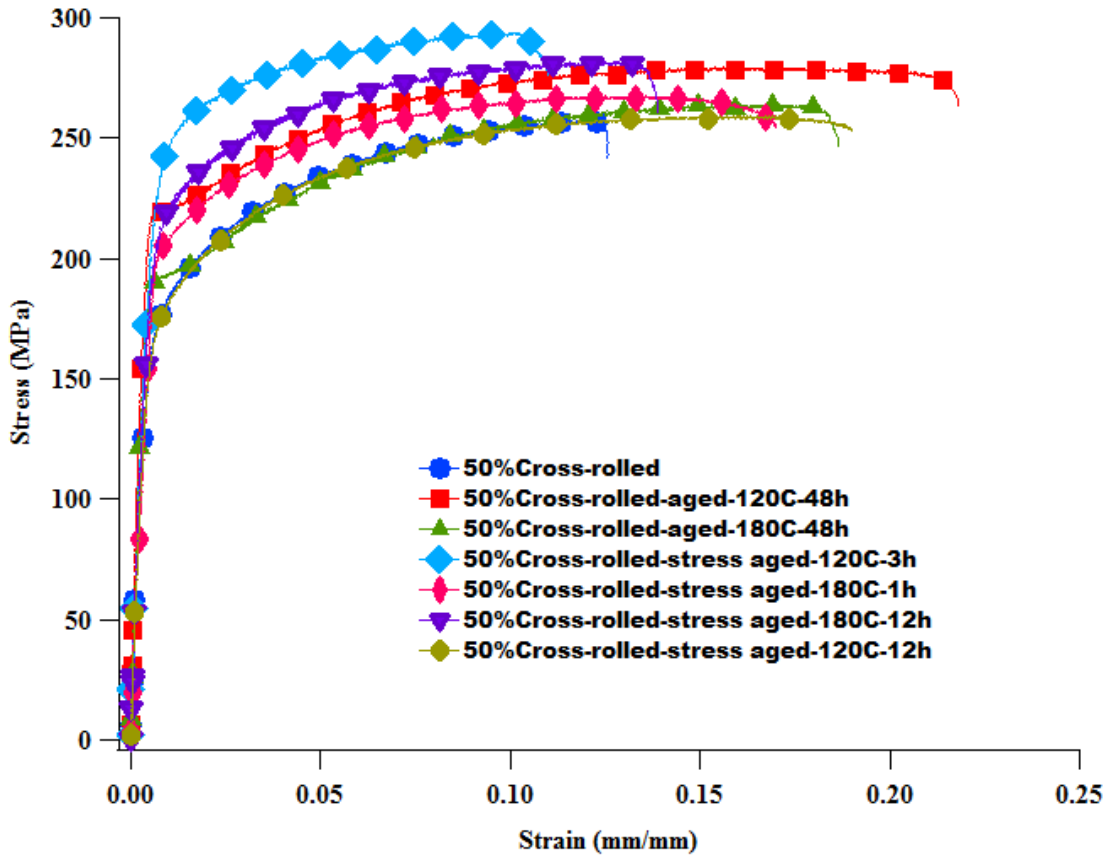

Figure 4.14 Stress-strain curves of 50% cross-rolled AZ31 after different aging conditions.

Although the conventional aging at 180˚C was not much more effective on the strength of the cross-rolled sample and only increased the ductility up to 18% after 48h, the aging treatment at 120˚C enhanced the yield and ultimate strength significantly up to 200MPa and 265MPa, respectively. Additionally, ductility of the sample after 48h aging at 120˚C was increased to 22% (Fig. 4.14).

Otherwise, stress aging was more effective to improve the strength of the cross-rolled samples and after 3h stress aging at 120˚C, the ultimate strength was increased up to about 300MPa with the expense of a reduction in ductility to 11%. Furthermore, stress aging at 180˚C for 12h increased the yield and UTS of the samples up to 270MPa without

a major change in ductility but fort he sample aged at 120˚C for 12h ductility improvement can be observed without enhancement in the strength of the sample.

4.4 Fracture morphology

The tensile fracture surface of AZ31 magnesium alloy for different conditions is shown in Fig. 4.15. The surface is characterized by cleavage facets and steps represents a relatively brittle fracture mechanism for all conditions. The fracture surface of the as-received sample with a high density of tears and remarkable small dimples depicts a completely different fracture manner with the rolled conditions (Fig. 4.15a).

On the other hand, Fig. 4.15b demonstrates mixed fracture modes, consists of intergranular fracture of small recrystallized grains and fast fracture of coarse grains formed throughout the grain growth of rolled sample during the aging treatment. It can be attributed to the enhanced precipitation hardening during the dynamic aging heat treatment for this sample.

Also, increasing the duration of aging treatment at 120 °C, from 24 h to 48 h, enhanced the density of tears on the fracture surface due to the grain growth of the samples and existence of the coarse grains in the microstructure of samples after 48 h aging (Fig. 4.15c, d). The similar trend was observed for the samples aged at 180°C (Fig. 4.15c, d). But as shown in Fig.4.15f, the fast fracture occurred on the cleavage facets prevented the development of dimples on the fracture surface.

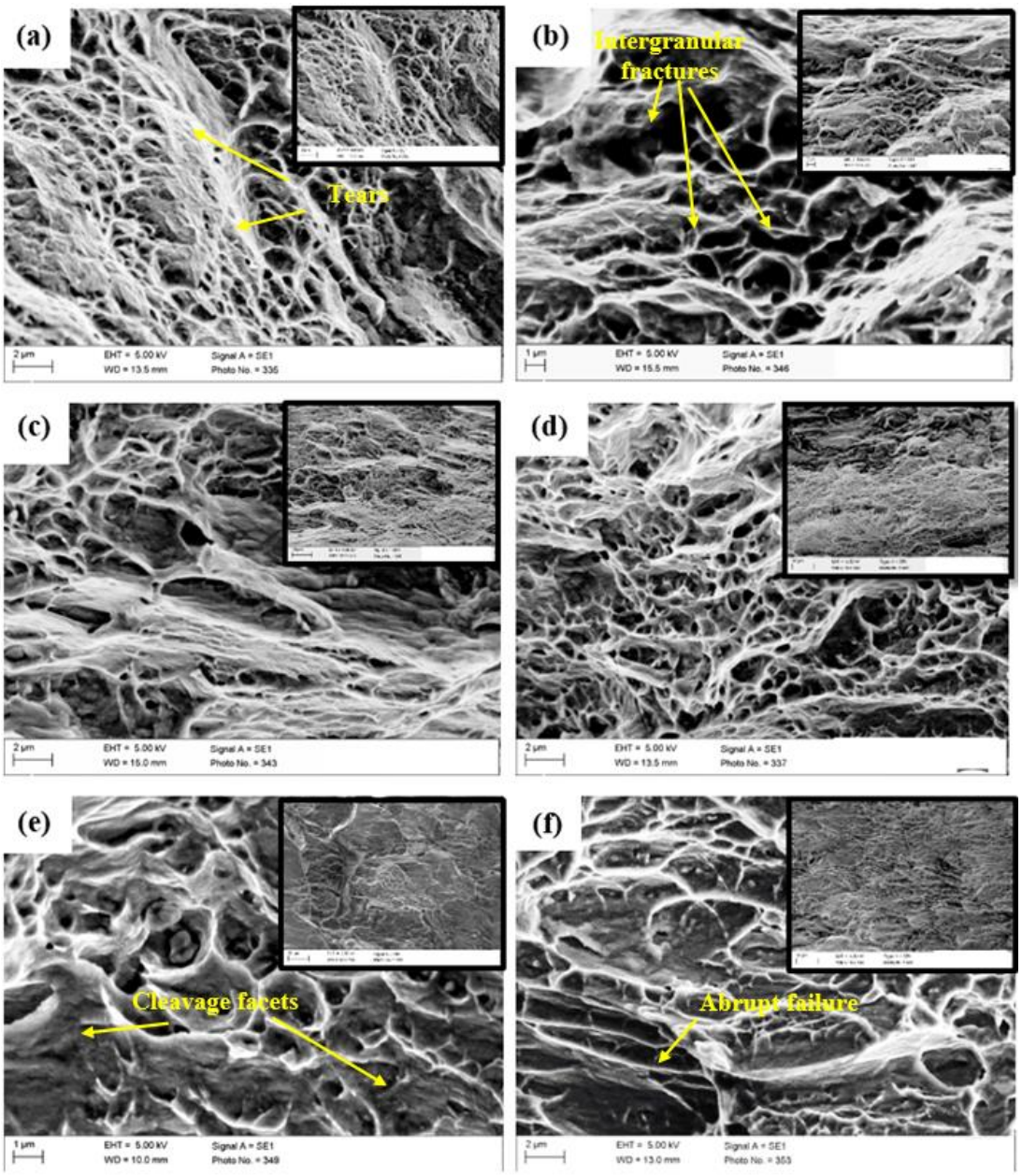

Figure 4.15 Fracture surface of the AZ31 magnesium alloy for different conditions of (a) as-received; (b) 75% rolled then stress aged under 50 MPa at 120˚C for 1 h; 75% rolled then conventional aged at (c) 120˚C for 24 h; (d) 120˚C for 48 h; (e) 180˚C for 24 h; (f) 180˚C for 48 h; (Insets represent the low magnification images of each condition).

4.5 Thermal Conductivity

The thermal conductivity test results for different conditions of AZ31 magnesium alloy samples are shown in Table. 4.2. The standard deviations of the mean value of the achieved results listed in Table 4.2 were smaller than 1%.

Table 4.2 Thermal conductivity test results.

Conditions	**Specific heat capacity** (Cp)	**Density (g/cm3)** (ρ)	**Thickness (mm)**	**Thermal diffusion** (α)	**Thermal Conductivity (W/mK)** (λ)
ST (as-received)	0.999	1.783	1.124	48.456	86.365
ST-Cross rolled 50%, Stress Aged-50Mpa,120ºC,3h	0.924	1.761	1.161	45.759	74.437
ST-Cross rolled 50%, Aged-180º,12h	1.026	1.731	1.016	46.450	82.454
ST-Rolled 75%, Stress Aged 50Mpa,120ºC,1h	1.191	1.835	1.164	45.408	99.239
ST-Rolled 75% Aged-120ºC,24h	1.091	1.774	1.072	46.467	89.944

The highest level of thermal conductivity was achieved after stress aging under the stress level of 50 MPa for at 120 ºC for 1h. It can be attributed to the precipitation hardening of AZ31 under the stress aging which affects the density, thermal diffusivity, and specific heat capacity of AZ31 samples.

5 CONCLUSIONS

In the current study, warm rolling followed by conventional aging and stress aging was performed on an AZ31 magnesium alloy. The mechanical properties of prepared materials were investigated by hardness, uniaxial tensile test, microstructure, fracture surface, and thermal conductivity observations.

The results of tensile tests revealed that aging at 120 °C for 24 h after 75% rolling enhanced the UTS of material to 300 MPa. besides, 48 h aged sample at 120 °C recovered the ductility after rolling and enhanced the strain up to 13% due to the nucleation of recrystallized grains, followed by growth of new grains. Similarly, aging the rolled sample at 180 °C for 24 h enhanced the ductility up to 14% with the expense of reduction of YS down to 180 MPa as attributed to the coarser grains of the aged sample.

Furthermore, stress aging method developed the yield strength of the as-received sample to 240 MPa without significant negative effect on the ductility in a short aging time of 1 h. This strength improvement was linked to the acceleration of precipitation hardening through the stress aging and consequently particle-stimulated nucleation.

Toughness of the samples were calculated using the area of stress-strain curves and results revealed that absorbed energy for the samples with high ductility was higher than the others. Accordingly, the highest toughness values were detected for the sample aged at 180 °C for 48 h and sample stress aged at 120 °C for 3 h.

In addition, fracture morphology of rolled samples depicts a brittle fracture surface with cleavage facets, while a mixture of intergranular fracture of small recrystallized grains and fast fracture of coarse grains fracture mechanisms was observed for stress aged sample. Also, high density of tears was observed on the fracture surface of conventionally

aged samples after 48 h and fast fracture of coarse grains prevented the creation of dimples.

Furthermore, the thermal conductivity after stress aging process at 120˚C for 1h was increased up to 99 W/mK as attributed to the favorable precipitate formations during stress aging.

Finally, the mechanical response of AZ31 magnesium alloy after conventional and stress aging were investigated and the optimum conditions of heat treatment were detected to improve the mechanical properties of the mentioned alloy.

6 FUTURE WORKS

Although some efforts were made to study the microstructure and mechanical behavior of warm rolled AZ31 magnesium alloy after aging and stress aging in the current work, these approaches are not restricted to the performed experiments and attained results. Thus, a few suggestions for future investigations are listed below:

1. The effect of stress aging on the fatigue performance of the AZ31 for high cycle fatigue and low cycle fatigue need to be investigated to characterize the cyclic mechanical behavior of stress aged samples.

2. High-temperature mechanical behavior of the AZ31 after stress aging process needs to be investigated to realize the performance at elevated temperatures.

VITA

Mustafa Misirli was born in 1988 in Keşan. He received his B.Sc. in Mechanical Engineering from Dokuz Eylül University, Turkey in 2012 and he is currently pursuing the M.Sc. degree in Mechanical Engineering at Ozyegin University with MEMFIS research group. His research interest mainly includes the mechanical properties of light alloys. Also, he is working as a Design Architect in the R&D department of Vestel Electronics. He is a member of Mechanical Design Group and he is a specialist for the mechanical design of LED televisions.

REFERENCES

[1] L.L. Rokhlin, Magnesium alloys containing rare earth metals: structure and properties, Crc Press2003.

[2] G. Lorimer, Z. Yang, J. Li, J. Zhang, G. Lorimer, J. Robson, Review on research and development of magnesium alloys, 21(5) (2009) 313-328.

[3] I. Ostrovsky, Y. Henn, Present state and future of magnesium application in aerospace industry, International Conference “New Challenges in Aeronautics”, Moscow, 2007.

[4] G.L. Song, A. Atrens, Corrosion mechanisms of magnesium alloys, Advanced engineering materials 1(1) (1999) 11-33.

[5] M.M. Avedesian, H. Baker, ASM specialty handbook: magnesium and magnesium alloys, ASM international1999.

[6] F. Von Buch, J. Lietzau, B. Mordike, A. Pisch, R. Schmid-Fetzer, Development of Mg–Sc–Mn alloys, Materials Science and Engineering: A 263(1) (1999) 1-7.

[7] F.W. Bach, M. Schaper, C. Jaschik, Influence of lithium on hcp magnesium alloys, Materials Science Forum, Trans Tech Publications Ltd., Zurich-Uetikon, Switzerland, 2003, pp. 1037-1042.

[8] G. Eger, Studies on the constitution of the ternary Mg-Al-Zn alloys, Int Z Metallographie 4 (1913) 50-128.

[9] E.F. Emley, Principles of Magnesium Technology (Oxford, New York, Pergamon Press, 1966).

[10] H. Palaniswamy, G. Ngaile, T. Altan, Finite element simulation of magnesium alloy sheet forming at elevated temperatures, Journal of Materials Processing Technology 146(1) (2004) 52-60.

[11] F.C. Campbell, Lightweight Materials: Understanding the Basics, ASM International2012.

[12] I. Polmear, Magnesium alloys and applications, Materials science and technology 10(1) (1994) 1-16.

[13] Q.-F. Chang, D.-Y. Li, Y.-H. Peng, X.-Q. Zeng, Experimental and numerical study of warm deep drawing of AZ31 magnesium alloy sheet, International Journal of Machine Tools and Manufacture 47(3) (2007) 436-443.

[14] D. Hull, D.J. Bacon, Introduction to dislocations, Butterworth-Heinemann2001.

[15] J. Koike, R. Ohyama, T. Kobayashi, M. Suzuki, K. Maruyama, Grain-boundary sliding in AZ31 magnesium alloys at room temperature to 523 K, Materials Transactions 44(4) (2003) 445-451.

[16] J. Koike, Enhanced deformation mechanisms by anisotropic plasticity in polycrystalline Mg alloys at room temperature, Metallurgical and Materials Transactions A 36(7) (2005) 1689-1696.

[17] J. Koike, T. Kobayashi, T. Mukai, H. Watanabe, M. Suzuki, K. Maruyama, K. Higashi, The activity of non-basal slip systems and dynamic recovery at room temperature in fine-grained AZ31B magnesium alloys, Acta materialia 51(7) (2003) 2055-2065.

[18] L. Shang, Effect of microalloying on microstructure and hot working behavior for AZ31 based magnesium alloy, 2008.

[19] P. Partridge, The crystallography and deformation modes of hexagonal close-packed metals, Metallurgical reviews 12(1) (1967) 169-194.

[20] G.E. Dieter, D.J. Bacon, Mechanical metallurgy, McGraw-hill New York1986.

[21] A. Ghaderi, M.R. Barnett, Sensitivity of deformation twinning to grain size in titanium and magnesium, Acta materialia 59(20) (2011) 7824-7839.

[22] Y. Chen, L. Jin, J. Dong, Z. Zhang, F. Wang, Twinning effects on the hot deformation behavior of AZ31 Mg alloy, Materials Characterization 118 (2016) 363-369.

[23] Y. Jiang, Y.a. Chen, Y. Wang, Compound role of tension twins and compression twins in microstructure and mechanical properties of Mg-Sn-Li rod, Materials Science and Engineering: A 682 (2017) 31-37.

[24] G. Liu, R. Xin, X. Shu, C. Wang, Q. Liu, The mechanism of twinning activation and variant selection in magnesium alloys dominated by slip deformation, Journal of Alloys and Compounds 687 (2016) 352-359.

[25] P. McGhee, Effect of Microstructure on the Mechanical Properties of Extruded Magnesium and a MagnesiumAlloy, North Carolina Agricultural and Technical State University, 2017.

[26] L. Whitmore, J. Denk, G.A. Zickler, G. Bourret, O. Huber, N. Huesing, O. Diwald, Macro to nano: a microscopy study of a wrought magnesium alloy after deformation, European Journal of Physics (2019).

[27] U.F. Kocks, C.N. Tomé, H.-R. Wenk, Texture and anisotropy: preferred orientations in polycrystals and their effect on materials properties, Cambridge university press2000.

[28] L. Chang, E. Shang, Y. Wang, X. Zhao, M. Qi, Texture and microstructure evolution in cold rolled AZ31 magnesium alloy, Materials characterization 60(6) (2009) 487-491.

[29] A. Lavakumar, Mechanical properties of materials, Concepts in Physical Metallurgy, Morgan & Claypool Publishers, 2017, pp. 5-1-5-22.

[30] F.J. Humphreys, M. Hatherly, Recrystallization and related annealing phenomena, Elsevier2012.

[31] I. Persechino, Development of a polycrystal plasticity simulation tool including recrystallization (DRX) phenomena, 2017.

[32] S. Yoo, S. Han, W. Kim, Magnesium matrix composites fabricated by using accumulative roll bonding of magnesium sheets coated with carbon-nanotube-containing aluminum powders, Scripta Materialia 67(2) (2012) 129-132.

[33] Q. Wang, X. Xiao, J. Hu, W. Xu, X. Zhao, S. Zhao, An ultrafine-grained AZ31 magnesium alloy sheet with enhanced superplasticity prepared by accumulative roll bonding, Journal of Iron and Steel Research, International 14(5) (2007) 167-172.

[34] J. Del Valle, M.T. Pérez-Prado, O.A. Ruano, Texture evolution during large-strain hot rolling of the Mg AZ61 alloy, Materials Science and Engineering: A 355(1-2) (2003) 68-78.

[35] J. Gao, S. Guan, Z. Ren, Y. Sun, S. Zhu, B. Wang, Homogeneous corrosion of high pressure torsion treated Mg–Zn–Ca alloy in simulated body fluid, Materials Letters 65(4) (2011) 691-693.

[36] B. Bonarski, E. Schafler, B. Mingler, W. Skrotzki, B. Mikulowski, M. Zehetbauer, Texture evolution of Mg during high-pressure torsion, Journal of materials science 43(23-24) (2008) 7513-7518.

[37] K. Matsubara, Y. Miyahara, Z. Horita, T. Langdon, Developing superplasticity in a magnesium alloy through a combination of extrusion and ECAP, Acta materialia 51(11) (2003) 3073-3084.

[38] H. Lin, J. Huang, T. Langdon, Relationship between texture and low temperature superplasticity in an extruded AZ31 Mg alloy processed by ECAP, Materials Science and Engineering: A 402(1-2) (2005) 250-257.

[39] M.T. Pérez-Prado, O. Ruano, Grain refinement of Mg–Al–Zn alloys via accumulative roll bonding, Scripta materialia 51(11) (2004) 1093-1097.

[40] S. Jayalakshmi, R. Singh, M. Gupta, Metallic Glasses as Potential Reinforcements in Al and Mg Matrices: A Review, Technologies 6(2) (2018) 40.

[41] A.P. Zhilyaev, T.G. Langdon, Using high-pressure torsion for metal processing: Fundamentals and applications, Progress in Materials science 53(6) (2008) 893-979.

[42] K. Edalati, Z. Horita, A review on high-pressure torsion (HPT) from 1935 to 1988, Materials Science and Engineering: A 652 (2016) 325-352.

[43] P.W. Bridgman, Effects of High Shearing Stress Combined with High Hydrostatic Pressure, Physical Review 48(10) (1935) 825-847.

[44] W.J. Kim, J.K. Kim, T.Y. Park, S.I. Hong, D.I. Kim, Y.S. Kim, J.D. Lee, Enhancement of strength and superplasticity in a 6061 Al alloy processed by equal-channel-angular-pressing, Metallurgical and Materials Transactions A 33(10) (2002) 3155-3164.

[45] K. Nakashima, Z. Horita, M. Nemoto, T.G. Langdon, Influence of channel angle on the development of ultrafine grains in equal-channel angular pressing, Acta materialia 46(5) (1998) 1589-1599.

[46] H.E. Friedrich, B.L. Mordike, Technology of magnesium and magnesium alloys, Magnesium Technology: Metallurgy, Design Data, Applications (2006) 219-430.

[47] M.-H. Sha, G.-D. Shi, W. Yu, Q. Jun, Paint-bake response of AZ80 and AZ31 Mg alloys, Transactions of Nonferrous Metals Society of China 20 (2010) s571-s575.

[48] H.T. Jeong, T.K. Ha, Texture development in a warm rolled AZ31 magnesium alloy, Journal of Materials Processing Technology 187 (2007) 559-561.

[49] J.-F. Nie, Precipitation and hardening in magnesium alloys, Metallurgical and Materials Transactions A 43(11) (2012) 3891-3939.

[50] R.E. Smallman, R.J. Bishop, Modern physical metallurgy and materials engineering, elsevier1999.

[51] Y. Uematsu, K. Tokaji, M. Matsumoto, Effect of aging treatment on fatigue behaviour in extruded AZ61 and AZ80 magnesium alloys, Materials Science and Engineering: A 517(1) (2009) 138-145.

[52] N. Hansen, Hall–Petch relation and boundary strengthening, Scripta Materialia 51(8) (2004) 801-806.

[53] Y. Wang, H. Choo, Influence of texture on Hall–Petch relationships in an Mg alloy, Acta Materialia 81 (2014) 83-97.

[54] J. Yuan, K. Zhang, X. Zhang, X. Li, T. Li, Y. Li, M. Ma, G. Shi, Thermal characteristics of Mg–Zn–Mn alloys with high specific strength and high thermal conductivity, Journal of Alloys and Compounds 578 (2013) 32-36.

[55] S.F. Corbin, D.M. Turriff, Thermal diffusivity by the laser flash technique, Characterization of Materials (2002) 1-10.

[56] S. Lee, H.J. Ham, S.Y. Kwon, S.W. Kim, C.M. Suh, Thermal conductivity of magnesium alloys in the temperature range from− 125 C to 400 C, International Journal of Thermophysics 34(12) (2013) 2343-2350.

[57] T.-C. Chang, J.-Y. Wang, C.-M. O, S. Lee, Grain refining of magnesium alloy AZ31 by rolling, Journal of Materials Processing Technology 140(1) (2003) 588-591.

[58] P. Sepehrband, M. Lee, A. Burns, Pre-Straining Effect on Precipitation Behaviour of AZ31B, Magnesium Technology 2016, Springer2016, pp. 89-92.

[59] F. Guo, D. Zhang, X. Yang, L. Jiang, F. Pan, Strain-induced dynamic precipitation of Mg17Al12 phases in Mg–8Al alloys sheets rolled at 748K, Materials Science and Engineering: A 636 (2015) 516-521.

[60] X. Li, F. Jiao, T. Al-Samman, S. Ghosh Chowdhury, Influence of second-phase precipitates on the texture evolution of Mg–Al–Zn alloys during hot deformation, Scripta Materialia 66(3) (2012) 159-162.

[61] A. Singh, H. Somekawa, T. Mukai, Compressive strength and yield asymmetry in extruded Mg–Zn–Ho alloys containing quasicrystal phase, Scripta Materialia 56(11) (2007) 935-938.

[62] J.D. Robson, D.T. Henry, B. Davis, Particle effects on recrystallization in magnesium–manganese alloys: Particle pinning, Materials Science and Engineering: A 528(12) (2011) 4239-4247.

[63] M. Mabuchi, K. Higashi, Strengthening mechanisms of Mg- Si alloys, Acta Materialia 44(11) (1996) 4611-4618.

[64] J.D. Robson, D.T. Henry, B. Davis, Particle effects on recrystallization in magnesium–manganese alloys: Particle-stimulated nucleation, Acta Materialia 57(9) (2009) 2739-2747.

[65] L. Troeger, E. Starke Jr, Particle-stimulated nucleation of recrystallization for grain-size control and superplasticity in an Al–Mg–Si–Cu alloy, Materials Science and Engineering: A 293(1-2) (2000) 19-29.

[66] J. Robson, D. Henry, B. Davis, Particle effects on recrystallization in magnesium–manganese alloys: Particle-stimulated nucleation, Acta Materialia 57(9) (2009) 2739-2747.

[67] J. Koehler, The nature of work-hardening, Physical Review 86(1) (1952) 52.